A Quasi-Equilibrium Tropical Circulation Model—Formulation*

J. DAVID NEELIN AND NING ZENG

Department of Atmospheric Sciences and Institute of Geophysics and Planetary Physics, University of California, Los Angeles, Los Angeles, California

(Manuscript received 1 July 1998, in final form 13 May 1999)

ABSTRACT

A class of model for simulation and theory of the tropical atmospheric component of climate variations is introduced. These models are referred to as quasi-equilibrium tropical circulation models, or QTCMs, because they make use of approximations associated with quasi-equilibrium (QE) convective parameterizations. Quasi-equilibrium convective closures tend to constrain the vertical temperature profile in convecting regions. This can be used to generate analytical solutions for the large-scale flow under certain approximations. A tropical atmospheric model of intermediate complexity is constructed by using the analytical solutions as the first basis function in a Galerkin representation of vertical structure. This retains much of the simplicity of the analytical solutions, while retaining full nonlinearity, vertical momentum transport, departures from QE, and a transition between convective and nonconvective zones based on convective available potential energy. The atmospheric model is coupled to a one-layer land surface model with interactive soil moisture and simulates its own tropical climatology. In the QTCM version presented here, the vertical structure of temperature variations is truncated to a single profile associated with deep convection. Though designed to be accurate in and near regions dominated by deep convection, the model simulates the tropical and subtropical climatology reasonably well, and even has a qualitative representation of midlatitude storm tracks.

The model is computationally economical, since part of the solution has been carried out analytically, but the main advantage is relative simplicity of analysis under certain conditions. The formulation suggests a slightly different way of looking at the tropical atmosphere than has been traditional in tropical meteorology. While convective scales are unstable, the large-scale motions evolve with a positive effective stratification that takes into account the partial cancellation of adiabatic cooling by diabatic heating. A consistent treatment of the moist static energy budget aids the analysis of radiative and surface heat flux effects. This is particularly important over land regions where the zero net surface flux links land surface anomalies. The resulting simplification highlights the role of top-of-the-atmosphere fluxes including cloud feedbacks, and it illustrates the usefulness of this approach for analysis of convective regions. Reductions of the model for theoretical work or diagnostics are outlined.

1. Introduction

a. Quasi-equilibrium tropical circulation model approach

A class of model for the tropical circulation is proposed that exploits the constraints placed on the flow by convective parameterizations with quasi-equilibrium (QE) thermodynamic closures. These models are thus referred to as quasi-equilibrium tropical circulation models (QTCMs). The essence of this class of models is that part of the QE convective closure can be used to carry forward analytically the model solution for the vertical structure in convective regions. These analytical solutions can then be used to construct a numerical scheme tailored to the interaction of convection with large-scale dynamics. Because part of the solution has been carried out analytically, the leading part of the solution can be captured by relatively few simple equations. This helps provide theoretical insight into the moist dynamics of the tropical circulation and can provide a sequence of intermediate models of this circulation that can be evaluated at successive levels of accuracy. The derivation of analytical solutions for convective regions, and examination of theoretical implications for tropical motions, have been carried forward in an ongoing project (Neelin and Yu 1994, hereafter NY94; Yu and Neelin 1997, hereafter YN97; Yu et al. 1998, hereafter YCN) that is summarized in Neelin (1997, hereafter N97). The first of a number of versions of these QTCMs is presented here. The simplest version is chosen that adequately simulates primary features of

* University of California, Los Angeles, Institute of Geophysics and Planetary Physics Contribution Number 5096.

Corresponding author address: Dr. J. David Neelin, Department of Atmospheric Sciences, University of California, Los Angeles, Los Angeles, CA 90095-1565.
E-mail: neelin@atmos.ucla.edu

the tropical climatology to illustrate the approach and because this version suggests insights into aspects of tropical atmospheric dynamics, especially with regard to atmosphere–land and atmosphere–ocean interactions. We also discuss examples of further simplifications of this QTCM to facilitate analysis of tropical dynamics.

At the heart of QE convective closures is the assertion that convective ensembles at scales smaller than the Reynolds average (sub-Reynolds scales) tend to remove convective instability within the vertical column (conditional instability of the first kind), establishing a statistical equilibrium between the variables that affect parcel buoyance, that is, the large-scale temperature and moisture, when an ensemble average is taken over a convective region (see Arakawa 1993; Emanuel 1994). How this is defined varies; for instance, in the Arakawa–Schubert (Arakawa and Schubert 1974) scheme, buoyancy (as measured by the Arakawa cloud-work function) is removed for each entraining cloud type, while for the Betts–Miller scheme (Betts 1986; Betts and Miller 1986, 1993, hereafter Betts–Miller) the closure amounts to removing convective available potential energy (CAPE) or a very closely related quantity. Traditional convective adjustment searches for parcel instability in the column and then adjusts temperature to a convectively neutral profile (Manabe and Strickler 1964; Manabe et al. 1965). The Betts–Miller scheme is an example of a smoothly posed moist convective adjustment scheme that has a small but finite timescale for the establishment of QE by sub-Reynolds convection. This permits some departure from QE conditions even in convective regions. A distinction is made between ''strict QE,'' in which QE closure constraints are applied stringently for all timescales, and QE that allows effects of finite adjustment time. Other schemes that relax toward QE rather than impose strict QE include Moorthi and Suarez (1992) and Randall and Pan (1993), both using the Arakawa–Schubert framework. Emanuel et al. (1994) have argued that using the QE approximation as an approach to thinking about tropical dynamics provides insight into how convection influences the large-scale flow and avoids pitfalls associated with conceptually separating the convective heating from the thermodynamics of the large-scale flow.

The QE constraints can apply to the flow only so long as convective criteria are met for some part of the time–space domain under the Reynolds average. They will thus tend to be most useful in regions where the large-scale dynamics (including evaporation and radiative cooling) are tending to produce convective instability, and where it is realistic to assume that, for large enough timescales and space scales, the sub-Reynolds scales are establishing a statistical equilibrium. Although this holds over a substantial part of the Tropics, an important issue is how to make use of QE constraints to simplify the solution, while incorporating nonconvective regions and departures from QE in convective regions. Examples of analytical solutions that apply where specific strict QE conditions hold (for deep convection, using the Betts–Miller scheme), and for simplified linear cases, is given in NY94 and YN97. Here we show how to make use of QE constraints in a more general framework.

There are two stages in the derivation of QTCMs: 1) finding near-analytical solutions or components of solutions that hold under reasonable approximations when the system is in QE and 2) embedding these solutions in a numerical framework so that the model can be used under conditions where the analytical solutions no longer apply. After establishing notation for the primitive equations and convective scheme in section 2, in section 3a, we repeat a summary of the analytical solutions from N97 to motivate the subsequent approach. We then use vertical structures based on these analytical solutions as the leading basis functions in a Galerkin projection. This approach with ''tailored basis functions'' is outlined in section 3b. By projecting the primitive equations onto these structures, self-consistent nonlinear terms can be retained in advection, moist convection, and vertical momentum transfer terms, among others. We will use the term QTCM to refer to models that retain a relatively complete representation of such effects from the primitive equations, as projected on the retained structures from the QE solution. Further approximations based on QE considerations are, of course, possible (some are discussed here, and some have been discussed in YN97), but we do not refer to such versions as QTCMs.

For the model presented here, we use a severe truncation of the vertical structures, retaining only one basis function for the vertical structure of temperature (which implies two for velocity). Where it is necessary to denote specifically this model version, we use the term QTCM1, associated with the number of retained vertical temperature structures. Because the vertical structures of temperature, wind, and vertical velocity are based on solutions under QE conditions, we argue that they carry a large fraction of the solution in and near convective regions. Section 3c discusses means by which additional information about physical processes and vertical structure can sometimes be extracted using approximation methods. Section 4 gives an outline of the model derivation (details in appendix A), along with considerations of the physical parameterizations needed for modeling tropical climate, such as a streamlined longwave radiation scheme from Chou and Neelin (1996, hereafter CN96). Section 4 has the equations in a form permitting some generalization, for instance, for moisture closure or surface stress parameterization, for future work. The hurried reader can skip directly to section 5, which has a relatively self-contained summary of the equations for this model version.

One of the motivations for this model is to have an intermediate atmospheric model adequate for theoretical studies of land–atmosphere interaction, and a land surface representation is needed for simulation of realistic tropical climate. The basic elements of a land surface

scheme appropriate for this level of model are outlined in section 6, while a more in-depth presentation is given in Zeng et al. (2000, hereafter ZNC). Section 7 discusses model properties. A number of interesting properties of the tropical atmosphere can be deduced from inspection of the model equations (section 7a). A taste of the model's simulation of the tropical climatology aids further discussion of these properties (section 7b); more detailed examination of the climatology and interannual variability is deferred to ZNC. Some consequences for land–atmosphere interaction that can be seen directly from the equations are noted in section 7c, while simplifications that could be applied to the model for analysis or simplified theory are noted in section 7d. Section 8 provides summary and discussion.

b. Relationship to simpler models and to GCMs

Since deep convection is such an important process in tropical dynamics, even simple models of tropical flow have to deal with it somehow. Most theoretical or simple modeling work has avoided complex convective closures and used extremely simplified representations of convection. Most commonly, these fix the vertical structure of convective heating, with its magnitude taken proportionally to moisture convergence, or simply to low-level convergence with a tunable coefficient. Such schemes are referred to here as convergence feedback parameterizations. They are sometimes referred to as CISK (conditional instability of the second kind) parameterizations since they can lead to instabilities in the large-scale model flow. The view of the tropical circulation associated with such models has had a strong influence upon the field, especially for large-scale tropical internal variability [e.g., Hayashi (1970); Lindzen (1974); Stevens and Lindzen (1978); Crum and Stevens (1983); Lau and Peng (1987); Hendon (1988); Wang (1988); Sui and Lau (1989); Bladé and Hartmann (1993); Wang and Li (1994); see Stevens et al. (1997) for historical review]. Convergence feedback schemes have also been used to examine the response of the tropical atmosphere to sea surface temperature (SST) boundary conditions, for which case most work has been done with very few vertical layers, usually with no moisture equation, and often with semiempirical linkages of convective heating to SST. Nonetheless, these models appear to give useful simulations of anomalous tropical low-level winds (Gill 1980; Webster 1981; Zebiak 1986; Lindzen and Nigam 1987; Neelin and Held 1987; Kleeman 1991; Wang and Li 1993; Zeng et al. 1996). One by-product of the current modeling effort is to seek justification for why such simple models can work, using a model with a more detailed representation of deep convection. This also permits an assessment of the limitations of such simple models. YN97 provide some discussion of this in a QE context.

The convergence feedback schemes, if applied in a multilevel model, show considerable sensitivity to the assumed vertical structure of the convective heating (e.g., Stevens and Lindzen 1978; Seager and Zebiak 1994). Work with QE schemes suggests that the vertical structure of the heating actually adapts strongly to balance the other terms in the large-scale temperature and moisture equations (NY94; Emanuel 1998). Indeed if the vertical structure of the heating is fixed, it is far from clear that the model has more than one vertical degree of freedom, as far as interaction of convection with large-scale dynamics is concerned, even if many levels are employed in discretizing the dry dynamics. For instance, YCN note that the effective static stability of the tropical atmosphere shows sensitivity to vertical variations in the depth of convection. In regions with large low-level moist static energy, convection tends to extend through a deeper layer, and the resulting increase in adiabatic cooling keeps the atmosphere stable for large-scale motions. Convergence feedback parameterizations usually omit this crucial effect. The observed vertical structure of heating also changes considerably among different flow regimes (Yanai and Johnson 1993).

How many vertical degrees of freedom in, say, temperature, are effectively represented in QTCM1, with one temperature basis function, compared to a GCM discretized by level but running the same Betts–Miller convective scheme? In the limit of small convective adjustment time, for conditions dominated over a sufficient region by deep convection, the QTCM solution should compare closely in that region with the GCM even for a large number of levels. Far from convective regions, for instance in midlatitudes, QTCM1 is qualitatively similar to a two-level model with a single temperature level. Overall, however, we would argue that QTCM1 is not merely a two-level model with carefully estimated parameters. It is a model that has asymptotic solutions in the vertical in convective regions compared to a GCM running the Betts–Miller convective adjustment. The solution is just done in two stages; the first stage is done in advance of the time integration, so the time-integrated stage is fast.

Seager and Zebiak (1994, 1995) examine the behavior of the Betts–Miller scheme in a linear primitive-equation model. Their approach is complementary to this since their model is more similar to a GCM in that the dry dynamics is treated separately from the moist dynamics. Our approach differs in actually using the constraints from the moist dynamics in building the model. This aids in theoretical interpretation of the moist dynamics. Since they retain more conventional vertical degrees of freedom, comparison to their model can provide a cross-check for ours. Also complementary are theoretical approaches like that of Rodwell and Hoskins (1996) where dry dynamics of descent regions are examined in detail, while moist convective effects are essentially given by specifying tropical diabatic heating or divergence sources. The present model trades off

vertical resolution of regions of absolute descent to focus on the effects of interaction with convection.

In terms of representing a tropical climate solution, the success or limitations must be demonstrated in practice. However, it seems important to introduce a model that occupies a niche between GCMs and simple models, in which the derivation from the primitive equations is done step by step, stating approximations systematically, and in which the convective scheme has a clear relation to a GCM convective scheme. The QTCM approach occupies this niche, and QTCM1 aims to do it in a manner that facilitates analysis of phenomena by shoehorning as much physics as possible into a few crucial vertical degrees of freedom.

This being said, caveats must be underlined: the assumption that convection produces an equilibrium profile is quite strong (in GCMs as well as here). By the reduction in vertical degrees of freedom, there will inevitably be phenomena for which the model is not appropriate. The applicability will undoubtedly be dependent on the horizontal scale and timescale of the phenomena, and there is no clear way of telling a priori where the limitations will be encountered. Quasi-equilibrium assumptions must fail at small scales, for which convective ensembles cease to be meaningful, and where convective and mesoscale motions are driven by release of CAPE. If the present approach can capture and give insight into some large-scale phenomena, it at least provides a relatively simple starting point in dealing with the complexity of tropical flow.

2. Notation and convective closure

a. Primitive equations

The standard nonlinear primitive equations provide the basis for the model. We summarize them here, with approximations stated later as appropriate. The region of focus is the troposphere below the highest convective heating.

The thermodynamic and moisture equations have the form

$$(\partial_t + \mathcal{D}_T)T + \omega\partial_p s = Q_c + g\partial_p R^{\uparrow} - g\partial_p R^{\downarrow} - g\partial_p S + g\partial_p F_T \tag{2.1}$$

$$(\partial_t + \mathcal{D}_q)q + \omega\partial_p q = Q_q + g\partial_p F_q, \tag{2.2}$$

where T is temperature in energy units (i.e., with the heat capacity at constant pressure C_p absorbed); q is moisture in energy units (i.e., with the latent heat per unit mass, L, absorbed); and $s = T + \phi$ is the dry static energy, with ϕ the geopotential. Here, $R^{\uparrow}$ and $R^{\downarrow}$ are the upward and downward longwave radiative heating heating fluxes as nonlocal functions of the temperature, moisture, and cloudiness over the column, signed in the direction of the flux. Net shortwave radiative flux is S, signed downward; and $S = S^{\downarrow} - S^{\uparrow}$, where $S^{\downarrow}$ and $S^{\uparrow}$ are downward and upward components, respectively. The operators $\mathcal{D}_T$ and $\mathcal{D}_q$ include horizontal diffusion and horizontal advection terms. We use

$$\mathcal{D}_T = \mathcal{D}_q = \mathbf{v}\cdot\boldsymbol{\nabla} - K_H\nabla^2. \tag{2.3}$$

The vertical fluxes of sensible heat and moisture by nonmoist-convective turbulent transport (parameterized as diffusion), F_T and F_q, have surface sensible heating and evaporation terms, H and E, as boundary conditions at the surface and vanish at model top. The ''convective heating'' and ''moistening'' terms are Q_c and Q_q.

The momentum equations combined with the hydrostatic equation are

$$(\partial_t + \mathcal{D}_V)\mathbf{v} + f\mathbf{k}\times\mathbf{v} + g\partial_p\boldsymbol{\tau} = -\boldsymbol{\nabla}\int_p^{p_{rs}} \kappa T\, d\ln p - \boldsymbol{\nabla}\phi_s, \tag{2.4}$$

where ϕ_s is the geopotential at the surface reference pressure level, p_{rs}, and

$$\mathcal{D}_V = \mathbf{v}\cdot\boldsymbol{\nabla} + \omega\partial_p - K_H\nabla^2 \tag{2.5}$$

is an operator with advection terms (including curvature terms) and horizontal diffusion terms. Vertical fluxes of horizontal momentum (''stress'' hereafter) are denoted $\boldsymbol{\tau}$. Gravitational acceleration is g. The ratio $\kappa = R/C_p$, where R is the gas constant for air, appears in the hydrostatic equation since T has absorbed C_p. Changes in water vapor create slight variations in κ. In later derivations, we neglect horizontal gradients, allowing it to be a function of pressure for a reference basic state.

Mass continuity is used in the form

$$\omega = \omega_s + \int_p^{p_s} \boldsymbol{\nabla}\cdot\mathbf{v}\, dp \tag{2.6}$$

$$\omega_s \approx -\rho_a g\mathbf{v}_s\cdot\boldsymbol{\nabla}z_s, \tag{2.7}$$

where z_s is surface elevation, p_s is surface pressure, ρ_a is atmospheric near-surface density, and $\rho_a d\phi_s/dt$ has been neglected. For the version derived here, we will omit topography for simplicity of presentation; that is, we will approximate

$$\omega_s = 0 \tag{2.8}$$

and take $p_s \approx p_{rs}$. The simplest extension to include topography is given in appendix A. The upper-boundary condition

$$\omega_t = 0 \tag{2.9}$$

is applied at $p = p_{rt}$. In the full primitive equations, this applies at $p = 0$; since no stratosphere is included in this model version, ideally (2.9) should be replaced by a condition approximating vertical radiation of planetary wave energy.

Boundary conditions for stress in the momentum equations are zero stress at model top and a bulk formula parameterization for surface drag:

$$\tau|_{p=p_t}| = 0, \tag{2.10}$$

$$\tau_s = \tau|_{p_s} = \rho_a C_D \mathrm{V}_s \mathbf{v}_s, \tag{2.11}$$

where $\mathbf{v}_s$ is the surface wind and V_s is the surface mean wind speed, parameterized on the large-scale surface or near-surface wind. Further discussion of the surface drag parameterization is given in section 4e.

The stress within the atmosphere due to turbulent eddy mixing is parameterized as a viscosity, much as in GCM simulations:

$$\tau = -\nu \partial_p \mathbf{v}, \tag{2.12}$$

with ν a function of p and possibly a function of $\mathbf{v}$ and stratification. The sign is chosen such that surface stress is positive for downward transfer of westerly momentum.

An important subsidiary constraint is moist energy conservation in the column, which holds for all convective schemes:

$$\hat{Q}_c + \hat{Q}_q = 0, \tag{2.13}$$

where $\widehat{(\,)}$ denotes vertical averaging over the troposphere, as defined in (2.16), with convective heating assumed confined below the tropopause.

This implies a vertically integrated moist static energy equation

$$\partial_t(\hat{T} + \hat{q}) + \widehat{\mathcal{D}_T T} + \widehat{\mathcal{D}_q q} + \widehat{\omega \partial_p h} = (g/p_T)F^{\mathrm{net}}, \tag{2.14}$$

where the moist static energy is $h = s + q$. The net flux into the atmospheric column is

$$F^{\mathrm{net}} = S_t^{\downarrow} - S_t^{\uparrow} - S_s^{\downarrow} + S_s^{\uparrow} - R_t^{\uparrow} - R_s^{\downarrow} + R_s^{\uparrow} + E + H, \tag{2.15}$$

where subscripts t and s on the solar and longwave radiative terms denote surface and model top, and $R_t^{\downarrow} \approx 0$ has been used. Bulk formulas for evaporation E and sensible heat flux H are discussed in section 4e.

Vertical averages over the troposphere are here defined as

$$\hat{X} = \langle X \rangle = p_T^{-1} \int_{p_{rt}}^{p_{rs}} X \, dp, \tag{2.16}$$

where the near-surface reference level p_{rs} is used rather than surface pressure p_s, to avoid horizontal derivatives of limits of integration. For the same reason, a constant tropopause reference level, p_{rt}, is defined (such that convective heating is confined below p_{rt}). Likewise, $p_T = p_{rs} - p_{rt}$ is a constant reference pressure depth of the troposphere. The actual pressure at the top of the convective heating will be denoted p_t, which can be a function of space and time. Since inner products will be the same as vertical averages in all cases considered here, $\langle X \rangle$ and $\hat{X}$ are used interchangeably.

b. Convective closure

1) Convective heating

The approach and implications explored here depend on convection tending to constrain the vertical structure of the temperature field. Moist convective adjustment (MCA; Manabe and Strickler 1964) is the simplest QE scheme since it makes this constraint on the temperature field explicit. Numerical implementations of MCA sometimes adjust the temperature profile discontinuously at the model time step. An improved MCA was proposed by Betts (1986) and Betts and Miller (1986, 1993), which is smoothly posed, parameterizing the convection as adjusting the column over a finite time τ_c. This is a measure of the timescale on which convective elements tend to reduce CAPE in the column. This timescale is usually considered to be less than a day; Betts and Miller (1986) used 2 h. In the Betts–Miller scheme, strict QE would be the limit $\tau_c \to 0$.

The form of the convective heating for this smoothly posed convective adjustment may be written

$$Q_c = \begin{cases} (T^c - T)/\tau_c, & \text{if } \langle T^c - T \rangle > 0 \\ 0, & \text{otherwise,} \end{cases} \tag{2.17}$$

where T^c is a convective QE profile toward which convection adjusts the temperature profile. It depends on the planetary boundary layer (PBL) moist static energy, assuming deep convection to arise out of the PBL. To a first approximation the T^c profile can be thought of as a moist adiabat rising from the PBL, but modifications due to freezing/melting, etc., can be included. To satisfy the energy constraint (2.13), the vertical integral of T^c must be suitably adjusted. Here we use a variant of Betts–Miller that takes into account some effects of adjustments to PBL moist static energy by downdrafts. This is related in spirit to a version discussed by Betts and Miller (1993), though not identical.

Let h_b be the PBL moist static energy. The vertical dependence of the moist adiabat does not change rapidly with h_b, so T^c can be expanded about a reference state QE profile, $T_r^c(p)$ as

$$T^c = T_r^c(p) + A_1(p) T_1^c, \tag{2.18}$$

where

$$T_1^c = h_b' + \delta h_b. \tag{2.19}$$

The reference profile T_r^c is independent of time and horizontal position, and it is split off for accuracy since it does not appear in any time or horizontal derivative terms. Here h_b' denotes departures of PBL moist static energy from this QE reference profile, and $A_1(p)$ gives the vertical shape of the moist adiabat perturbation per h_b perturbation. Below the reference lifting condensation level, $A_1(p)$ is a dry adiabat. The quantity δh_b is an adjustment to the boundary layer moist static energy by downdrafts. In Betts (1986) a vertically constant correction term is used, but here we assume that the deep

convective motions arise following $A_1(p)$ from a boundary layer that has been adjusted by an amount to be determined by other parts of the closure. In fact, for the case discussed here, T_1^c is determined directly, as seen below, and δh_b need only be calculated as a diagnostic (equivalently, N97 simply redefines h_b as the adjusted value).

Linearization of the dependence of the moist adiabat on h_b in (2.18) holds well within the Tropics, but the nonlinearity can also be hidden in $A_1(p)$. Note that (2.17) is nonlinear in either case due to the requirement that the vertically integrated heating be nonnegative. When applied in the temperature equation, the closure (2.17) tends to reduce a modified measure of CAPE, as defined relative to T^c. Adjustment is here specified to occur whenever the vertical integral of $T^c - T$ is positive, that is, whenever there is CAPE under this measure.

The important part of this heating closure is that in convective regions, temperature tends to be constrained toward the convective QE profile T^c. Other QE schemes will also tend to have this property, although the QE temperature profile T^c may not be given explicitly. The specific case presented here using the Betts–Miller deep convective scheme could be generalized in future model versions, so long as the QE temperature profiles under typical conditions can be expressed with relatively few vertical degrees of freedom:

$$T^c = T_r^c(p) + \sum_{k=1}^{N} T_k^c A_k(p), \tag{2.20}$$

where N is small, T_k^c are scalar coefficients, and $A_k(p)$ the few basis functions needed to capture most T^c variations.

2) Convective moisture closure

The moisture closure is treated separately here since the most essential results depend on the form of the temperature closure. The moisture closure could potentially be considerably generalized within this model framework. For Betts–Miller, the moisture closure has the form [in regions where heating is nonzero according to (2.17)]

$$Q_q = (q^c - q)/\tau_c, \tag{2.21}$$

where q^c is an assumed convective QE profile for moisture. This can be written as

$$q^c = \alpha_{\text{sub}} q_{\text{sat}}(T^c), \tag{2.22}$$

where $\alpha_{\text{sub}}(p)$ is a subsaturation coefficient, which can vary in the vertical. For current purposes we need only a smooth adjustment toward a moisture profile that can be found for given temperature and moisture in the column. For the case where T, q are close to T^c, q^c, and where T^c is given by (2.18), we can postulate a closure where the q^c for deep convection depends only on the QE temperature profile. For simplicity, we use here a linear form of this dependence, giving

$$q^c = q_r^c(p) + B_1(p) T_1^c, \tag{2.23}$$

where $B_1(p)$ is the vertical profile for deep convective QE moisture variations. Effects of alternate closures are discussed in further work (H. Su et al. 2000, personal communication), including a case in which the moisture closure can be greatly relaxed by changing the assumptions on δh_b so neither (2.22) nor (2.23) is required. The nonlinear q^c temperature dependence in (2.22) proves important to quantitative aspects of midlatitude simulation, but the linearized form of it (2.23) is used here and in ZNC to demonstrate that it can be adequate for many purposes.

3. Motivation and tailored basis functions

a. Summary of approximate solutions in deep convective regions

Motivation for the approach taken here comes from previous work showing the strong simplifications of the flow that QE constraints produce in convective regions. NY94 obtained analytical solutions for primitive equations and Betts–Miller convective heating linearized about a radiative–convective equilibrium, oriented toward intraseasonal modes of variability. YN97 examined this linearized case for steady circulations, using a crude Rayleigh friction for momentum damping, while N97 extended these results to keep a number of nonlinear terms. Here we summarize the essential aspects of the analytical solutions for our approach. They are obtained under the following approximations. (i) Convection keeps temperature sufficiently close to the QE profile that baroclinic temperature gradients are dominated by the QE component. (ii) Baroclinic advection and vertical transport of momentum are neglected in the momentum equations. These approximations are relaxed in the QTCM derivation in section 3b.

If T is constrained to be close to the QE profile T^c, we can replace T by T^c in the baroclinic pressure gradients. Using (2.18) (and $\nabla T_r^c = 0$), and replacing $\mathcal{D}_V$ with an approximation $\tilde{\mathcal{D}}_V$, the momentum (with hydrostatic) equation (2.4) becomes

$$\begin{aligned}(\partial_t + \tilde{\mathcal{D}}_V)\mathbf{v} + f\mathbf{k} \times \mathbf{v} &= -\kappa \nabla \int_p^{p_{rs}} T^c \, d \ln p - \nabla \phi_s \\ &= -\kappa \int_p^{p_{rs}} A_1(p) \, d \ln p \nabla T_1^c - \nabla \phi_s. \end{aligned} \tag{3.1}$$

Thus baroclinic pressure gradients have strongly constrained vertical structure. Neglecting vertical diffusion, and retaining only barotropic advection in $\tilde{\mathcal{D}}_V$, analytical solutions can be obtained for velocity. Under these approximations, the operator on the lhs is independent of pressure, so components of the **v** solution must simply match vertical structures of the barotropic and baroclinic

pressure gradient terms. Each vertical structure in $\mathbf{v}$ implies a vertical structure of ω through the continuity equation (2.6). Using vertical boundary conditions $\omega = 0$ at the surface and the tropopause, (2.8)–(2.9), gives two solutions to (3.1): an unforced nondivergent barotropic solution, and a baroclinic solution in which the boundary conditions link ϕ_s to the baroclinic pressure gradients.

The vertical structure of the baroclinic wind in deep convective regions in these approximate solutions is

$$\mathbf{v}(x, y, p, t) = V(p)\mathbf{v}_T(x, y, t),$$

$$V(p) = (A_1^+(p) - \widehat{A_1^+}), \quad \text{and}$$

$$A_1^+(p) = \int_p^{p_{rs}} A_1(\hat{p})\, d\ln\hat{p}, \tag{3.2}$$

where the vertical structure in $A_1^+(p)$ simply comes from the hydrostatic equation, integrating QE temperature vertical structure to give baroclinic pressure gradients. The continuity equation can be solved for the vertical structure $\Omega(p)$ of vertical velocity from the baroclinic wind (choosing signs such that Ω is positive):

$$\omega(x, y, p, t) = -\Omega(p)\nabla\cdot\mathbf{v}_T(x, y, t) \quad \text{and}$$

$$\Omega(p) = -\int_p^{p_{rs}} V(\hat{p})\, d\hat{p}. \tag{3.3}$$

The separation of velocity components in the vertical in (3.2) results from vertical coherence of the temperature structure, and thus of baroclinic pressure gradients, due to the effects of convection. In the analytical solutions, it implies that the solution for $\mathbf{v}_T$ involves only horizontal and time dependence. The implied vertical structure for ω in (3.3) yields simplifications in the thermodynamics when applied in the moist static energy equation (2.14). This becomes

$$\partial_t(\widehat{A_1}T_1^c + \hat{q}) + \langle\mathcal{D}_T A_1\rangle T_1^c + \langle\mathcal{D}_q q\rangle + M\nabla\cdot\mathbf{v}_T = (g/p_T)F^{\text{net}}, \tag{3.4}$$

where full nonlinearity has been retained and the moisture closure has not yet been used. Notably, a ''gross moist stability''

$$M = \langle\Omega(-\partial_p h)\rangle \tag{3.5}$$

arises that provides a net static stability for convergence of large-scale motions in convective regions, including the partial cancellation of adiabatic cooling by convective heating (see N97; YCN). Properties of this are discussed for the equivalent in QTCM1 in sections 5 and 7.

b. Tailored basis functions

The analytical solutions apply only in convective regions under certain approximations. We desire a model that preserves the useful aspects of the analytical solutions when these conditions apply but include (i) non-QE conditions, (ii) nonconvective regions, (iii) vertical momentum transfer by sub-Reynolds-scale turbulence and resulting surface stress, and (iv) full nonlinearity. Relative to the derivation of the previous section, this involves relaxing the approximations $T \approx T^c$ and $\mathcal{D}_V \approx \tilde{\mathcal{D}}_V$ in (3.1) among others.

Consider writing major variables in terms of a truncated series of basis functions in the vertical, as for a Galerkin expansion (or related projection methods):

$$T = T_r(p) + \sum_{k=1}^{K} a_k(p)T_k(x, y, t), \tag{3.6}$$

$$\mathbf{v} = \sum_{k=0}^{L} V_k(p)\mathbf{v}_k(x, y, t), \quad \text{and} \tag{3.7}$$

$$q = q_r(p) + \sum_{k=1}^{K} b_k(p)q_k(x, y, t). \tag{3.8}$$

For the dynamically active part of the solution, horizontal gradients and time derivatives of T, q matter, so splitting off a portion of the solution that does not depend on space or time $T_r(p)$, $q_r(p)$ can improve accuracy. These will be specified as a reference state, which is *not* assumed to be a solution, but which may be chosen to be close to the anticipated solution typical of deep convective regions.

It is common in Galerkin techniques to choose basis functions from an orthogonal series of relatively simple functions. Here the analytical solution is available as an asymptotic approximation as certain conditions are approached (short convective timescales and negligible vertical momentum transfer). We simply adopt the analytical solution as a leading basis function. Higher basis functions could, in principle, be constructed using orthogonality conditions and other criteria to continue the series. However, the interest here is to see how much of the solution can be captured with very few vertical degrees of freedom. In the simplest case presented here, a single vertical degree of freedom is used in T. Likewise, velocity basis functions are adopted from the analytical solution. In a more general case, a limited number of basis functions *tailored to the dominant physical processes*, in particular convective QE constraints, would be used. This approach is predicated on the assumption that convective QE constraints tend to reduce the number of vertical degrees of freedom that are crucial to the solution.

Here we choose as the leading basis function for temperature:

$$a_1(p) = A_1(p, T_r^c), \tag{3.9}$$

where $A_1(p)$ is the vertical structure of temperature changes associated with the leading convective adjustment profile in (2.20), to capture temperature structures associated with deep convective regions. Evaluation of A_1 at T_r^c is specified since nonlinear variations in A_1 could be included, though we omit them here, whereas a_1 appears in terms with spatial and time derivatives and

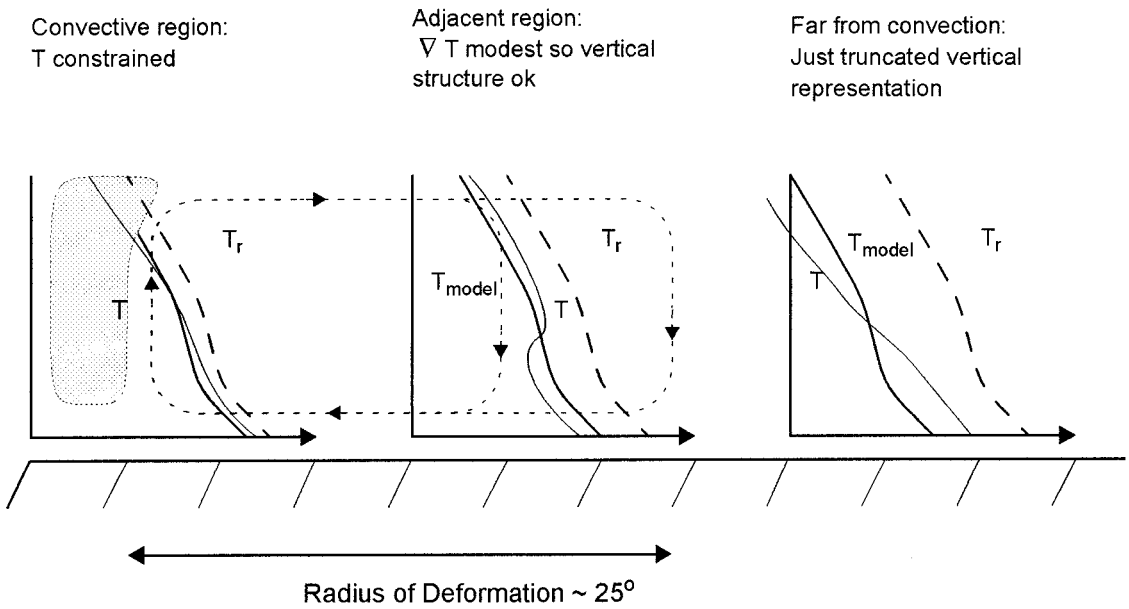

FIG. 1. Schematic of how the basis function for deep temperature structure chosen appropriately for a QE convective parameterization may be expected to approximate the solution when applied more generally. The solid curve indicates the model representation of temperature, $T_{\text{model}} = T_r + a_1(p)T_1$, where the reference profile T_r is independent of space and time (dashed curve). In convective regions, T_{model} tends to be close to actual temperature T (thin curve) since both are close to the convective QE temperature (not shown). Far from convective regions, T_{model} matches the vertical average of T, but vertical structure may deviate.

so would yield complications if not strictly a function of p. Choosing

$$V_1(p) = a_1^+ - \widehat{a_1^+} \tag{3.10}$$

captures the velocity field associated with baroclinic pressure gradients due to such temperature variations, where a_1^+ is defined just as for A_1^+ in (3.2).

Considering (3.1) for the case $T_1^c = 0$ shows that a solution component must also be included for the barotropic component of the motions. A basis function

$$V_0(p) = 1 \tag{3.11}$$

captures this.

While the choice of temperature and velocity basis functions are closely linked, discretization of the moisture equation is largely independent. We choose a truncation for the moisture equation to have a similar level of complexity as for the temperature equation, but this could be relaxed. If using the moisture closure (2.23), one might consider using

$$b_1(p) = B_1(p), \tag{3.12}$$

which would be well suited for convective regions. However, for climate modeling, other considerations are important for moisture, in particular, behavior in low-moisture regions in the subtropics. We thus leave b_1 general in the derivations. A choice that handles low-moisture regions gracefully is

$$b_1(p) = q_r(p)/q_r(p_s). \tag{3.13}$$

When total moisture becomes small, this avoids the problem of some levels having negative moisture when fields are reconstructed from the projected equations. Using (3.12) can overestimate radiative contributions of upper-tropospheric water vapor in the subtropics, since B_1 tends to be moist over a greater depth than occurs in the subtropics. This can affect ocean-coupling applications. The normalization of b_1 in (3.13) does not affect the physics, but simply scales q_1 (note, however, that the longwave radiative coefficient of moisture contributions must use the same normalization). In numerical results presented here and in Zeng et al. (1999), (3.12) is used; ZNC use (3.13).

Given that the temperature and velocity basis functions are derived for deep convective physics, why would projecting the equations on them in adjacent regions be useful? Temperature must vary smoothly in the horizontal, and atmospheric wave dynamics tends to spread temperature gradients out over a radius of deformation for off-equatorial regions, and even farther along the equator. Deep convection sets a deep temperature structure in the convection zones, and temperature in adjacent regions must adjust to this. For a typical dry, deep gravity wave phase speed of 55 m s^{-1}, the equatorial radius of deformation is about 26° of latitude. Hence, the temperature structure set by deep convective regions will tend to have considerable influence over much of the subtropics. Far from deep convective regions, the model simply becomes a highly truncated Galerkin representation. Figure 1 summarizes this ar-

gument schematically. The degree to which this holds depends, of course, on what competing processes might change vertical structure. Longwave radiation, a relatively slow process, is consistent with smooth vertical structures in the upper troposphere in descent regions. The most obvious processes producing deviations from this structure in the subtropics are boundary layer and shallow convective processes. To a certain extent, these are simply providing the near-surface heating that is not supplied by adiabatic descent to balance longwave cooling. Projection of the net effect of these processes onto a deep basis temperature basis function can thus be hoped to provide a viable approximation, as can be tested by attempting the simulation of tropical and subtropical climate. The approximation is further aided by the vertical integration of temperature in the pressure gradient term, so errors in temperature of small vertical scale tend to have relatively less effect on the dynamics. Vertical structures of moisture are not spread horizontally by gravity wave dynamics as occurs for temperature, so different considerations apply for the treatment of moisture.

There are many precedents for related methods. It is widely known that the efficiency of Galerkin techniques depends on the choice of basis functions for the problem at hand. In the early meteorological literature, there was discussion of using vertical structures based on empirical orthogonal functions (Holmström 1963). Galerkin vertical representation using finite elements has been employed in modeling both atmosphere (Staniforth and Daley 1977) and ocean (e.g., Song and Haidvogel 1994). McWilliams (1980) discussed projection of quasigeostrophic equations on a sequence of vertical basis functions for streamfunction. Use of empirical orthogonal functions in the horizontal has been shown by Selten (1997) to be inefficient due to the lack of fast transform methods for general basis functions because the number of basis functions required in the horizontal is large. We are not aware of previous work in which basis functions are chosen from asymptotic approximations, so the use of tailored basis functions is to some extent a novel variant. While Galerkin techniques commonly focus on convergence properties as the number of basis functions is increased, we are more concerned here with the question: given a good first approximation to the solution under some conditions, how good is the approximation at fixed truncation under slightly more general conditions? There is an obvious analogy with the method of normal forms (e.g., Guckenheimer and Holmes 1983), in which eigenvectors at a bifurcation are used to expand the nonlinear solution. The solution in that case is asymptotically accurate within some sufficiently small neighborhood of the bifurcation. The similarity is that both methods use spatial basis functions that are solutions under some conditions.

c. Approximation methods for remainder equations

Besides tailoring the leading basis functions to the physics, we deviate in another way from standard Galerkin methods. It is common to test accuracy, for instance, by increasing the number of basis functions; if truncation at N is sufficiently accurate, contributions to various terms of the equations by basis functions beyond N are negligible. In our equations, we have certain terms in which large parameters would make this a poor approximation for some aspects of the solution, and yet we desire to keep vertical degrees of freedom to a minimum. Fortunately, these same effects make approximation methods possible. Keeping track of the remainder solution beyond the retained basis functions, we write, for example, for T:

$$T = T_r(p) + \sum_{k=1}^{K} a_k(p)T_k(x, y, t) + T_R(x, y, p, t), \quad (3.14)$$

where T_R is the remainder solution for T. Conventionally, T_R would be assumed to be orthogonal to other terms in the expansion, and when multiplied by a variable or coefficient with a different vertical dependence, the resulting term would be assumed negligible. We likewise follow this procedure, except that we return to the remainder solution to seek next-order improvements where it is multiplied by a large parameter.

An important case is the convective heating term, where T_R is multiplied by τ_c^{-1}. The projected equations give accurate solutions for the temperature (especially when τ_c^{-1} is large) and other variables, but the vertical structure of the heating depends on the small difference $T^c - T$, multiplied by the large parameter. The vertical structure of the heating is thus diagnosed postsolution using the remainder equations, as outlined in appendix B. Although not exploited systematically in the current version, we conjecture that such approximations to remainder equations can be used to increase the amount of detail that can be included in a model that has fixed truncation in other respects. Climate models depend strongly on parameterized subgrid-scale processes, which tend to have different dependences than the large-scale dry dynamics. Wherever the subgrid-scale physics has a strong dependence on a detail of the solution that is otherwise negligible for the large-scale model, such next-order approximations for the remainder solution could potentially be included in the subgrid-scale parameterization.

4. Model derivation

This section provides enough of the derivation to provide a feel for how the physics is packed into a relatively simple final form of the model. Details are provided in appendix A. The resulting model in the form that is currently used is given in section 5, so users can skip this section if desired. This section also contains some results in a form more general than in section 5, to provide indications of possible model variants.

a. Continuity equation in the projected system

Having chosen basis functions for velocity, we desire vertical structures for vertical velocity consistent with mass conservation. Note that this is not simply a projection of the continuity equation. Rather, because vertical velocity is diagnostic in the primitive equations, mass continuity can be used to define its vertical structure. Integrating (2.6) for convergent motions associated with basis function V_1 (3.10) yields, similar to (3.3),

$$\omega_1(x, y, p, t) = -\Omega_1(p)\nabla \cdot \mathbf{v}_1(x, y, t) \quad \text{and}$$

$$\Omega_1(p) = -\int_p^{p_s} (a_1^+(\hat{p}) - \widehat{a_1^+})\, d\hat{p}. \tag{4.1}$$

Similarly, integrating (2.6) for convergent motions associated with V_0:

$$\omega_0 = \omega_t - \Omega\nabla \cdot \mathbf{v}_0, \qquad \Omega_0(p) = p - p_t, \tag{4.2}$$

with the total vertical velocity given by

$$\omega = \omega_0 + \omega_1. \tag{4.3}$$

Because $\langle V_1 \rangle = 0$, demanding that the continuity equation (2.6) be satisfied exactly in this truncated system implies

$$\nabla \cdot \mathbf{v}_0 = (\omega_t - \omega_s)/p_T. \tag{4.4}$$

Approximate effects of topography can be incorporated into the surface vertical velocity (appendix A) using the boundary condition (2.7). Likewise, it would be possible, in principle, to apply an approximation to a radiation condition, that is, upward-only propagation of wave energy into the stratosphere, to obtain ω_t as a function of other model variables (Yano and Emanuel 1991). Here we simply use (2.8), neglecting topography, and (2.9), neglecting vertical motion at the tropopause, so

$$\nabla \cdot \mathbf{v}_0 = 0. \tag{4.5}$$

b. Projection of momentum equations

Using V_0 and V_1 as the basis functions in the series (3.7), the momentum equations, including the $\partial_p \tau$ term, are projected onto these to obtain equations for $\mathbf{v}_0$ and $\mathbf{v}_1$ with truncation at $L = 1$. Taking the inner product of the momentum equation with V_0, and using (2.10)–(2.11),

$$\partial_t \mathbf{v}_0 + \mathcal{D}_{V0}(\mathbf{v}_0, \mathbf{v}_1) + f\mathbf{k} \times \mathbf{v}_0 + (g/p_T)\tau_s = -\nabla \phi_{s0}. \tag{4.6}$$

The operator containing nonlinear advection terms and horizontal diffusion is given by

$$\mathcal{D}_{Vk} = \sum_{i=0}^{1}\sum_{j=0}^{1} [D_{ijk}^{V}\mathbf{v}_i \cdot \nabla\mathbf{v}_j + D_{ijk}^{V\omega}(\nabla \cdot \mathbf{v}_i)\mathbf{v}_j] - K_H\nabla^2\mathbf{v}_k, \tag{4.7}$$

$$D_{ijk}^{V} = \langle V_i V_j V_k \rangle / \langle V_k^2 \rangle, \quad \text{and} \tag{4.8}$$

$$D_{ijk}^{V\omega} = \langle V_k \Omega_i \partial_p V_j \rangle / \langle V_k^2 \rangle. \tag{4.9}$$

For the case here, several elements of the sum are zero, so $\mathcal{D}_{V0}(\mathbf{v}_0, \mathbf{v}_1)$ and $\mathcal{D}_{V1}(\mathbf{v}_0, \mathbf{v}_1)$ are written explicitly in (5.11)–(5.12). The approach of calculating interaction coefficients for nonlinear terms as in (4.7)–(4.9) can be inefficient when large numbers of basis functions are included, but in this approach we only intend to work at low truncation.

We have defined

$$\phi_{s0} = \phi_s - \phi_{s1}, \tag{4.10}$$

which simply separates the component of surface geopotential associated with $\mathbf{v}_1$ from those associated with $\mathbf{v}_0$ solutions. The component of surface geopotential

$$\phi_{s1} = -\kappa\widehat{a_1^+}T_1 \tag{4.11}$$

arising from baroclinic motions is associated with the $\widehat{a_1^+}$ contribution to V_1 in (3.10). This is the component of barotropic motion needed for the directly baroclinically driven motions to satisfy boundary conditions of no vertical flow at the surface and tropopause. Neither is directly required in solution system; see appendix A for reconstruction of geopotential postsolution.

For vertical momentum transfer, the inner product has simply yielded the surface stress term in (4.6):

$$\langle V_0 \partial_p \tau \rangle = \langle \partial_p \tau \rangle = \tau_s/p_T.$$

In (4.12) we keep the presentation in terms of surface stress. Parameterization of this stress in terms of the wind field is discussed in section 4e.

Because $\mathbf{v}_0$ has a specified divergence (zero in cases without topography), it is determined by the vorticity equation

$$\partial_t \zeta_0 + \mathrm{curl}_z(\mathcal{D}_{V0}(\mathbf{v}_0, \mathbf{v}_1)) + \beta v_0 + f\nabla \cdot \mathbf{v}_0 = -(g/p_T)\,\mathrm{curl}_z \tau_s, \tag{4.12}$$

where β is the latitudinal derivative of f. Solution in terms of a streamfunction ψ_0 (such that $\mathbf{v}_0 = \mathbf{k} \times \nabla\psi_0$, $\zeta_0 = \nabla^2\psi_0$) reduces prognostic variables by one.

For the baroclinic component, taking the inner product of (2.4) with V_1 and normalizing by $\langle V_1^2 \rangle$ yields

$$\partial_t \mathbf{v}_1 + \mathcal{D}_{V1}(\mathbf{v}_0, \mathbf{v}_1) + f\mathbf{k} \times \mathbf{v}_1 = -\kappa\nabla T_1 - g\langle V_1^2 \rangle^{-1}[p_T^{-1}V_{1s}\tau_s + \langle \nu(\partial_p V_1)^2 \rangle \mathbf{v}_1]. \tag{4.13}$$

In the pressure gradient term, we have used (3.10) to derive $\langle V_1 \nabla \phi_s \rangle = \langle V_1 \rangle \nabla \phi_s = 0$, and $\langle V_1 \int_p^{p_s} \kappa T\, d\ln p \rangle = \langle V_1 a_1^+ \rangle \kappa \nabla T_1 = \langle V_1^2 \rangle \kappa \nabla T_1$. The vertical momentum transfer terms have been treated by integration by parts, as is customary for differentiated terms in Galerkin methods:

$$\langle V_1 \partial_p \tau \rangle = p_T^{-1}[V_1\tau]_0^{p_s} - \langle \tau \partial_p V_1 \rangle = p_T^{-1}V_{1s}\tau_s - \langle (-\nu\partial_p V_1)\partial_p V_1 \rangle \mathbf{v}_1.$$

The first term represents the effects, integrated over the column, of the vertical transfer of momentum onto surface stress. It is independent of the particular parame-

terization of turbulent momentum transfer. The second term is associated with turbulent mixing of shear in the baroclinic wind, and it does depend on the parameterization of mixing, here represented as an eddy viscosity. This term could be modified to include effects of momentum transfer by convection.

c. Projection of temperature equation

In the temperature and moisture equations, vertical mass-weighted integrals, that is, integrals in dp/g, are important to the moist static energy budget. It is desirable to maintain these in the projected equations. In the case treated here, truncated to a single basis function, it suffices to use a vertical integral (i.e., Petrov–Galerkin projection with unit test function). Possible choices for the more general case are outlined in appendix A. We maintain for this section the distinction between A_1 and a_1 because it tags terms arising from T^c and T, respectively, and because it would be feasible to include nonlinearity in A_1 that would be difficult to include in a_1. For most applications we will set $a_1 = A_1$.

Vertically averaging the temperature equation (2.1) yields

$$\hat{a}_1(\partial_t + \mathcal{D}_{T1})T_1 + M_{S1}\boldsymbol{\nabla}\cdot\mathbf{v}_1 = \epsilon_c(\widehat{T_r^c} + \hat{A}_1 T_1^c - \widehat{T_r} - \hat{a}_1 T_1) + (g/p_T)(-R_t^{\uparrow} - R_s^{\downarrow} + R_s^{\uparrow} + S_t - S_s + H), \quad (4.14)$$

where

$$\epsilon_c = \mathcal{H}(\widehat{T_r^c} + \hat{A}_1 T_1^c - \widehat{T_r} - \hat{a}_1 T_1)/\tau_c, \quad (4.15)$$

with $\mathcal{H}(\cdot)$ a heaviside function, here evaluated as a function of temperature departures from the convective QE profile to include the positive-only heating condition of (2.17). The difference $(\widehat{T_r^c} - \widehat{T_r})$ is maintained here for generality. For typical quantitative applications (ZNC), we take T_r^c as a moist adiabat arising from the boundary layer of T_r, q_r. However, the impact of shifting $\widehat{T_r}$ to equal $\widehat{T_r^c}$ is minimal, as illustrated in simulations presented here that use this simplification (see appendix A for further discussion of shifts in T_r). For theoretical applications, whichever choice is more convenient may be used. The nonlinear model, in any case, simulates heating from zero to large values; so small, spatially constant, reference state temperature differences are simply compensated by slight shifts in T_1 and q_1.

The operator $\mathcal{D}_{T1}$ contains projected nonlinear advection terms and horizontal diffusion and is given in (5.13). The projection of the QE temperature profile on a_1 is denoted T_1^c, given by (2.18). The flux terms on the right-hand side of the equation are defined following (2.1) and are here evaluated at the top and bottom of the tropospheric column, taking $R_t^{\downarrow} \approx 0$ and $F_{Tt} \approx 0$. Solar flux is written in terms of net downward flux, $S = S^{\downarrow} - S^{\uparrow}$; these downward and upward (reflected) components must be treated separately for applications considering land and cloud effects.

The dry static stability associated with the baroclinic wind convergence is

$$M_{S1} = p_T^{-1}\int_{p_{rt}}^{p_{rs}} \Omega_1(-\partial_p s)\, dp = M_{Sr1} + M_{Sp1}T_1(x, y, t), \quad (4.16)$$

where signs are chosen such that M_{S1} is positive, and where

$$M_{Sr1} = p_T^{-1}\int_{p_{rt}}^{p_{rs}} \Omega_1(p)(-\partial_p s_r(p))\, dp, \quad (4.17)$$

$$M_{Sp1} = p_T^{-1}\int_{p_{rt}}^{p_{rs}} \Omega_1(p)(-\partial_p s_1(p))\, dp, \quad \text{and} \quad (4.18)$$

$$\partial_p s_1(p) = \partial_p a_1 + \kappa a_1/p, \quad (4.19)$$

with s_1 the contribution to the dry static stability from a unit change of T_1. The gross dry stability has been split into a constant associated with the reference profile M_{Sr1} and a varying part where M_{Sp1} gives the change per T_1. This second term can be problematic in the midlatitude region of the model, where T_1 is cold, since the stratification is governed by different physics than in convective regions. In current implementations of the model, M_{S1} is kept constant outside of convective regions.

d. Projection of moisture equation and moisture closure

Vertically integrating the moisture equation (2.2) with vertical velocity and velocity truncated at V_1 yields, *before* expressing q in terms of basis functions,

$$\partial_t \hat{q} + \widehat{\mathcal{D}_q q} - M_{q1}\boldsymbol{\nabla}\cdot\mathbf{v}_1 = \langle Q_q\rangle + (g/p_T)E. \quad (4.20)$$

The term M_{q1} is the contribution to the gross moist stability by moisture convergence, termed the ''gross moisture stratification'' (NY94; YCN). It arises from the vertical integral of moisture convergence associated with $\mathbf{v}_1$ and is given by

$$M_{q1} = p_T^{-1}\int_{p_{rt}}^{p_{rs}} \Omega_1 \partial_p q\, dp, \quad (4.21)$$

with the sign chosen such that M_{q1} is positive. With T and $\mathbf{v}$ at current truncations, the main quantity by which q influences the rest of the dynamics is $\langle Q_q\rangle$ (aside from radiative terms and cloudiness parameterizations). Within the $\hat{q}$ equation, most quantities are weighted vertical integrals, except for near-surface moisture in the evaporation parameterization. This further motivates truncation of q vertical structure to a single basis function, $b_1(p)$, beyond the motivation provided in deep convective regions by the particular parameterization (2.23).

We note in appendix A that it is feasible to keep some limited variation of b_1 in the horizontal to increase accuracy at current truncation if needed. With $q = q_r + b_1 q_1$, M_{q1} is modified in the obvious way in (4.21), and the advection operator term in the projected moisture equation (5.4) becomes $\mathcal{D}_{q1} q_1$ as given in (5.14) or (A2).

Note that we have not yet used the moisture closure but have left $\langle Q_q \rangle$ to have a yet-to-be specified dependence on other variables. As underlined in N97, because the moisture closure is perhaps the least certain aspect of convective parameterizations, it is comforting that most of the important properties in the derivation do not depend on using it. The moisture closure will, of course, affect the simulation but has not so far affected the form of the model equations.

The energy constraint on convective heating and moisture sink (2.13) with the form of the convective heating (2.17) gives

$$\epsilon_c(\widehat{T_r^c} + \hat{A}_1 T_1^c - \widehat{T_r} - \hat{a}_1 T_1) + \langle Q_q \rangle = 0. \quad (4.22)$$

Once the moisture closure gives $\langle Q_q \rangle$ as a function of other large-scale variables, this determines T_1^c as a function of those variables. Because T_1^c is related by (2.19) to the PBL moist static energy adjusted such that the energy constraint holds ($h_b + \delta h_b$), (4.22) implies that the moisture closure may affect this adjustment process. The form (4.22) could be used to introduce a more general moisture closure, for instance, different constraints on h_b, or a modified cumulus mass flux scheme. Here we use the moisture closure (2.21), (2.23), and moisture truncated to a single basis function b_1 (potentially different than the QE moisture profile B_1). The convective moisture source becomes

$$\langle Q_q \rangle = \epsilon_c(\widehat{q^c} - \widehat{q_r} - \hat{b}_1 q_1). \quad (4.23)$$

The energy constraint (2.13) or (4.22) then implies

$$\hat{A}_1 T_1^c + \widehat{q^c} = \hat{a}_1 T_1 + \hat{b}_1 q_1 + \widehat{q_r} - (\widehat{T_r^c} - \widehat{T_r}). \quad (4.24)$$

This determines T_1^c in terms of T_1, q_1. The dependence of q^c on T_1^c is nonlinear if the version (2.22) of the moisture closure is used. No restrictions have yet been placed on the reference profile terms. The vertically averaged heating term in (4.14) and the moisture sink in (4.20) are given by

$$-\langle Q_q \rangle = \langle Q_c \rangle = \epsilon_c[\hat{A}_1 T_1^c - \hat{a}_1 T_1 + (\widehat{T_r^c} - \widehat{T_r})]. \quad (4.25)$$

In cases using the nonlinear moisture closure (2.22), the inverse of the nonlinear lhs of (4.24) may be precomputed to give T_1^c as a function of the rhs. For the linear moisture closure (2.23), the solution of (4.24) is

$$T_1^c = (\hat{A}_1 + \hat{B}_1)^{-1}[\hat{a}_1 T_1 + \hat{b}_1 q_1 - (\widehat{T_r^c} - \widehat{T_r}) - (\widehat{q_r^c} - \widehat{q_r})]. \quad (4.26)$$

In this case, (4.24) becomes

$$\begin{aligned} -\langle Q_q \rangle &= \langle Q_c \rangle \\ &= \epsilon_c \hat{A}_1 (\hat{A}_1 + \hat{B}_1)^{-1} \\ &\quad \times [\hat{b}_1 q_1 - \hat{B}_1 (\hat{a}_1 / \hat{A}_1) T_1 + (\hat{B}_1 / \hat{A}_1)(\widehat{T_r^c} - \widehat{T_r}) \\ &\quad - (\widehat{q_r^c} - \widehat{q_r})]. \end{aligned} \quad (4.27)$$

For the simplest case, setting $\hat{a}_1 = \hat{A}_1$, $\hat{b}_1 = \hat{B}_1$, $\widehat{T_r}$, $\widehat{T_r^c}$, and $\widehat{q_r} = \widehat{q_r^c}$, this reduces to (5.5), as discussed in section 5.

The term

$$C_1 = (\hat{A}_1 T_1^c - \hat{a}_1 T_1) + (\widehat{T_r^c} - \widehat{T_r}), \quad (4.28)$$

which in the simplest case is proportional to $(q_1 - T_1)$, is a measure of CAPE projected onto the retained basis functions. The projected CAPE increases as moisture increases, which is appropriate since moisture is concentrated at low levels. It increases as T_1 decreases as appropriate to cooling through a deep column. If comparing to observations, note that this measure of CAPE, while similar to the standard definition, differs in that it is defined for parcels rising from a value of the PBL moist static energy h_b that is adjusted so the energy constraint holds. It uses T^c as defined in the convective scheme, which need not be exactly a moist adiabat, as is used in the parcel ascent process by which standard CAPE is defined. To compare to standard CAPE, or for alternate moisture closures, one may use

$$h_b = T_r(p_{rs}) + T_1 a_1(p_{rs}) + q_r(p_{rs}) + q_1 b_1(p_{rs}). \quad (4.29)$$

The adjustment δh_b in (2.19) is determined implicitly by the moisture closure and could be calculated postsolution using (4.29).

e. Parameterization of surface fluxes

Bulk formulas for sensible heat over both land and ocean and for evaporation over ocean regions are

$$H = \rho_a C_H V_s (T_s - T_a) \quad \text{and} \quad (4.30)$$

$$E = \rho_a C_H V_s (q_{\text{sat}}(T_s) - q_a), \quad (4.31)$$

where T_s denotes the actual surface temperature, and T_a and q_a denote temperature and moisture in the atmospheric boundary layer just above the surface. The notation T_a is used to distinguish between near-surface and surface values in temperature; in variables for which there is no ambiguity, the subscript s is used. The near-surface air density ρ_a is approximated as constant. Evaporation over land regions is discussed in section 6.

Evaluating the solution based on retained basis functions at the surface leads to

$$T_a = T_r(p_s) + a_{1s} T_1, \; q_a = q_r(p_s) + b_{1s} q_1 \quad (4.32)$$

in (4.30) and (4.31), where $a_{1s} = a_1(p_s)$, and $b_{1s} = b_1(p_s)$. It would also be possible to include a simple model of an embedded boundary layer, if we assume boundary layer adjustment times fast compared to other timescales

and obtain a next-order correction to T_a and q_a, but the above is sufficient for many modeling purposes, and inclusion of an explicit boundary layer would lead to the next step up in the planned hierarchy of QTCMs.

The dependence of the bulk formula upon wind speed, especially in evaporation, turns out to be very important in the simulation of tropical climate. The drag coefficient and wind speed dependence are often estimated based on 10-m winds in observations, but the essence of the parameterization is that it gives the transfer coefficients for surface fluxes as a function of large-scale winds. For this model, we can use a parameterization for V_s (see appendix A) that takes into account the reduced vertical degrees of freedom in the explicitly modeled winds and the contribution of wind variations at space and timescales smaller than the Reynolds average.

For the specific parameterization of stress (2.10), the stress term in the $\mathbf{v}_0$ or ζ_0 equations (4.6) or (5.2) becomes, in terms of $\mathbf{v}_0$ and $\mathbf{v}_1$,

$$-(g/p_T)\tau_s = -\boldsymbol{\epsilon}_0\mathbf{v}_0 - \boldsymbol{\epsilon}_{10}\mathbf{v}_1, \tag{4.33}$$

while the stress term in the $\mathbf{v}_1$ equation (5.1) becomes

$$-g(\langle V_1^2\rangle)^{-1}[p_T^{-1}V_{1s}\tau_s + \langle\nu(\partial_p V_1)^2\rangle\mathbf{v}_1] = -\boldsymbol{\epsilon}_1\mathbf{v}_1 - \boldsymbol{\epsilon}_{01}\mathbf{v}_0. \tag{4.34}$$

Each of the momentum transfer coefficients $\boldsymbol{\epsilon}_0$, $\boldsymbol{\epsilon}_1$, $\boldsymbol{\epsilon}_{10}$, and $\boldsymbol{\epsilon}_{01}$, given in (5.15), contains nonlinear and spatial dependence. The term $\boldsymbol{\epsilon}_1$, which acts as a damping on the baroclinic wind component, in addition to the term due to transfer onto surface stress, has a term due to internal momentum transfer $\boldsymbol{\epsilon}_1 = \boldsymbol{\epsilon}_1^{\tau} + \boldsymbol{\epsilon}_1^{\text{int}}$. Interaction between the wind components due to surface stress, as governed by $\boldsymbol{\epsilon}_{10}$ and $\boldsymbol{\epsilon}_{01}$, is discussed in section 7a.

f. Radiation treatment and cloudiness parameterization

For longwave radiation, we employ the weakly nonlinear formulation of CN96, in which Green's functions for upward and downward longwave fluxes are calculated as a function of temperature and moisture for each of several cloud types, and for cloud fraction and cloud top for climatological temperature and moisture. From (4.14) we note that for a single temperature basis function, we require only $R_t^{\uparrow}$, $R_s^{\downarrow}$, and $R_s^{\uparrow}$ since these affect the atmospheric column balance. Projecting the Green's functions onto the retained basis functions in temperature and moisture gives a condensation of the CN96 scheme. Here we give the linearized case, with coefficients evaluated at a reference cloud fraction from Green's functions for each cloud type. ZNC give the weakly nonlinear version used in the numerical implementation:

$$\begin{aligned} R_t^{\uparrow} &= R_{rt}^{\uparrow} + \boldsymbol{\epsilon}_{RT_1t}^{\uparrow}T_1 + \boldsymbol{\epsilon}_{Rq_1t}^{\uparrow}q_1 + \sum_n \boldsymbol{\epsilon}_{R\alpha_n t}^{\uparrow}(\alpha_n - \alpha_{rn}) \\ &\quad + \boldsymbol{\epsilon}_{RT_st}^{\uparrow}(T_s - T_{rs}), \\ R_s^{\downarrow} &= R_{rs}^{\downarrow} + \boldsymbol{\epsilon}_{RT_1s}^{\downarrow}T_1 + \boldsymbol{\epsilon}_{Rq_1s}^{\downarrow}q_1 + \sum_n \boldsymbol{\epsilon}_{R\alpha_n s}^{\downarrow}(\alpha_n - \alpha_{rn}), \\ R_s^{\uparrow} &= R_{rs}^{\uparrow} + \boldsymbol{\epsilon}_{RT_ss}^{\uparrow}(T_s - T_{rs}), \end{aligned} \tag{4.35}$$

where α_n and α_{rn} are cloud fraction and reference cloud fraction, respectively, for cloud type n. The subscript r terms are longwave fluxes evaluated at the reference temperature, moisture, and cloud fraction profiles. The coefficients are calculated (before time integration) as

$$\boldsymbol{\epsilon}_{RT_1t}^{\uparrow} = \sum_n \alpha_{rn}\int_{p_{rt}}^{p_{rs}} G_T^{\uparrow n}(p_t, \dot{p})a_1(\dot{p})\,d\dot{p}, \tag{4.36}$$

with $G_T^{\uparrow n}$ the Green's function associated with general temperature perturbations for each cloud type n, and similarly for q_1 subscript and $\downarrow$ superscript. The T_1 terms in (4.35) appear similar to a Newtonian cooling, except that they are separated into upward and downward streams, as is essential for coupling to land or ocean. However, the greenhouse effect by the moisture term strongly modifies this in a highly spatially dependent manner, actually overcoming it in convective regions [see values in Table 1, noting $q_1 \approx T_1$ in convective regions using (5.5)]. The cloud term is locally much larger than either the T_1 or q_1 term, and it is linear by construction, since cloud types are defined to be nonoverlapping (CN96). The coefficients in (4.35) are in units of W m^{-2} K^{-1} for terms associated with temperature T_1 and moisture q_1 when both T_1 and q_1 are expressed in K; the coefficients are W m^{-2} for cloud fraction terms, with cloud fraction unitless. To convert the terms associated with temperature and moisture to inverse seconds, simply absorb the factor $(C_p p_T/g)^{-1}$ that multiplies these terms when (4.35) is applied in (5.3). The physical meaning of these rates should only be interpreted in suitable combinations.

The shortwave scheme is adapted from Chou (1997), as further described in ZNC. Variations due to surface and cloud albedo and atmospheric absorption are included.

As shown in Ockert-Bell and Hartmann (1992), CN96, and Chou (1997), a few cloud types can capture many essential features of the tropical radiation budget. A leading dependence, in which deep and cirrostratus/cirrocumulus (CsCc) clouds are linked to deep convective precipitation, is included in the runs presented in this paper. CsCc correlates well with deep convective clouds, and the regression coefficient is used to link the two; deep convective cloud, in turn, correlates well with precipitation following Chou (1997). The cloud fraction of the combined cloud types, α_1, is thus modeled as

$$\alpha_1 = c_{\alpha_1}\hat{Q}_c, \tag{4.37}$$

with the parameter c_{α_1} empirically determined. Additional details are given in ZNC. Ongoing work aims at

developing parameterizations for cirrus and stratus clouds appropriate for this level of model. In considering such parameterizations, it can be helpful to note that we have explicit vertical structures of variables in the retained basis functions and also that we can seek approximations to the remainder solutions, for instance, for the inversion in stratus regions.

5. Model summary

a. Main equations

For the standard version of QTCM1, with choices discussed in section 4, including $\hat{a}_1 = \hat{A}_1$, and the stress relation (4.33)–(4.34), the prognostic equations for barotropic wind component (4.12), baroclinic wind component (4.13), temperature (4.14), and moisture (4.20) become

$$\partial_t \mathbf{v}_1 + \mathcal{D}_{V1}(\mathbf{v}_0, \mathbf{v}_1) + f\mathbf{k} \times \mathbf{v}_1 = -\kappa \boldsymbol{\nabla} T_1 - \epsilon_1 \mathbf{v}_1 - \epsilon_{01} \mathbf{v}_0, \tag{5.1}$$

$$\partial_t \zeta_0 + \text{curl}_z(\mathcal{D}_{V0}(\mathbf{v}_0, \mathbf{v}_1)) + \beta v_0 = -\text{curl}_z(\epsilon_0 \mathbf{v}_0) - \text{curl}_z(\epsilon_{10} \mathbf{v}_1), \tag{5.2}$$

$$\hat{a}_1(\partial_t + \mathcal{D}_{T1})T_1 + M_{S1}\boldsymbol{\nabla} \cdot \mathbf{v}_1 = \langle Q_c \rangle + (g/p_T) \times (-R_t^{\uparrow} - R_s^{\downarrow} + R_s^{\uparrow} + S_t - S_s + H), \tag{5.3}$$

$$\hat{b}_1(\partial_t + \mathcal{D}_{q1})q_1 - M_{q1}\boldsymbol{\nabla} \cdot \mathbf{v}_1 = \langle Q_q \rangle + (g/p_T)E. \tag{5.4}$$

For the simplest case used in this paper, the moisture sink and convective heating terms are given by

$$-\langle Q_q \rangle = \langle Q_c \rangle = \epsilon_c^*(q_1 - T_1). \tag{5.5}$$

Forms for more general cases are given in section 4d. Results for the case (4.27) are shown in ZNC, while (4.25) with (4.24) can be used to improve midlatitude aspects. The simplest case (5.5) corresponds to setting $\hat{a}_1 = \hat{A}_1$, $\hat{b}_1 = \hat{B}_1$, $\widehat{T_r} = \widehat{T_r^c}$, and $\widehat{q_r} = \widehat{q_r^c}$ in (4.27). These choices do not greatly restrict the physical representation since they involve vertical integrals, not vertical structures.

b. Moist static energy equation

An alternate prognostic equation that is very useful in analyzing model dynamics is the moist static energy equation [the sum of (5.3) and (5.4)]:

$$\hat{a}_1(\partial_t + \mathcal{D}_{T1})T_1 + \hat{b}_1(\partial_t + \mathcal{D}_{q1})q_1 + M_1\boldsymbol{\nabla} \cdot \mathbf{v}_1 = (g/p_T)F^{\text{net}}. \tag{5.6}$$

This dominates the dynamics of convective regions, where the temperature and moisture equations alone have large canceling terms. It avoids fast, $O(\tau_c)$, timescales, which go into the adjustment of CAPE. It is very similar to the vertically integrated moist static energy equation of the primitive equations (2.14), balancing net flux into the column, F^{net}, against transport by the retained degrees of freedom. Although our coding uses separate T_1 and q_1 equations, it would be possible to run the model using (5.6) and either (5.3) or a CAPE equation formed from a suitably weighted difference of (5.3) and (5.4). Within convective regions, to the extent that QE ties q_1 to T_1, (5.6) contains all thermodynamic information necessary to solve for large scales, and this can be exploited to assist in understanding results. Some simplifications that occur over land, for instance, are discussed in section 7c.

c. Coefficients and operators

The form (2.21) with (2.23) has been used for Q_q, leading to the form for Q_c on the rhs of (5.3) [see (4.25)]. The positive-only nonlinearity is contained in ϵ_c, which from (4.15), is

$$\epsilon_c = \tau_c^{-1}\, \mathcal{H}(C_1). \tag{5.7}$$

The quantity $\mathcal{H}(C_1) = 0$, if $C_1 < 0$, $= 1$ if $C_1 > 0$ is a Heaviside function that represents the dependence of convection on conditional instability in the column. The quantity C_1 is a measure of CAPE for this model, projected on retained basis functions. It is given, in general, by (4.28), but for the simplest case (5.5), $C_1 \propto (q_1 - T_1)$. As discussed in section 4d, because T_1^c includes effects of feedbacks to the boundary layer, this is a modified measure of CAPE that satisfies the energy constraint on convective heating and moisture sink. For the simplest case, given in (5.5),

$$\epsilon_c^* \equiv \hat{a}_1\hat{b}_1\,(\hat{a}_1 + \hat{b}_1)^{-1}\,\epsilon_c \tag{5.8}$$

rescales the convective adjustment rate in the T and q equations.

The static stability terms are those associated with upper-level divergence (low-level convergence) of the baroclinic wind component: the dry static stability M_{S1}, the gross moisture stratification M_{q1}, and the gross moist stability M_1. These give, respectively, the work to raise a large-scale air mass, the resulting moisture convergence, and the net stratification resulting from adiabatic cooling minus diabatic heating in convective zones:

$$M_1 = M_{S1} - M_{q1}, \tag{5.9}$$

with the gross moisture stratification of (4.35) becoming

$$M_{q1} = M_{qr1} + M_{qp1}q_1, \qquad M_{qr1} = p_T^{-1}\int_{p_{rt}}^{p_{rs}} \Omega_1 \partial_p q_r\, dp,$$

$$M_{qp1} = p_T^{-1}\int_{p_{rt}}^{p_{rs}} \Omega_1 \partial_p b_1\, dp, \tag{5.10}$$

signed positive, and with M_{S1} given similarly by (4.30).

Note that while T_1 and q_1 are relative to reference values, the velocity and flux terms are total values. To

TABLE 1. Selected parameters and coefficients with typical values (some have spatial dependence or nonlinear dependence on other variables).

Term	Unit	Definition
$\hat{a}_1$, a_{1s}	0.38, 0.24 (unitless)	Vertical integral and surface value of temperature basis function
$\hat{b}_1$, b_{1s}	0.45, 0.61 (unitless)	Vertical integral and surface value of moisture basis function
V_{1s}	-0.20 (unitless)	Surface value of baroclinic wind basis function
C_D	0.9×10^{-3}, 3.7×10^{-3} (unitless)	Surface drag coefficient for ocean and forest
D^V_{110}, D^V_{111}	3.25×10^{-2}, 0.2	Coefficients $\langle V_1^2\rangle$, $\langle V_1^3\rangle/\langle V_1^2\rangle$ in the momentum advection operator
D^T_{111}, D^q_{111}	6.5×10^{-2}, -6.0×10^{-2}	Coefficients $\langle a_1 V_1\rangle/\hat{a}_1$, $\langle b_1 V_1\rangle/\hat{b}_1$ in the temperature and moisture advection operator associated with advection by baroclinic wind
τ_c	2 h	Convective adjustment time
$\epsilon_0(V_s)$, $\epsilon_1(V_s)$	$(5.6 \text{ day})^{-1}$, $(3.4 \text{ day})^{-1}$ for $V_s = 10$ m s^{-1}, $C_D = 10^{-3}$	Coefficient of projected vertical momentum transfer for barotropic and baroclinic wind components
$\epsilon_{10}(V_s)$, $\epsilon_{01}(V_s)$	$(-28 \text{ day})^{-1}$, $(-0.9 \text{ day})^{-1}$ for $V_s = 10$ m s^{-1}	Coefficients of transfer by surface stress between baroclinic and barotropic wind components in $\mathbf{v}_0$, $\mathbf{v}_1$ equation
$\epsilon_1^\tau(V_s)$, ϵ_1^{int}	$(4.53 \text{ day})^{-1}$, $(14.4 \text{ day})^{-1}$	Contributions to ϵ_1 by surface stress and internal mixing
$\epsilon^{\uparrow}_{RT_1t}$, $\epsilon^{\downarrow}_{RT_1s}$	0.9, 1.2 W m^{-2} K^{-1}	Longwave coefficients for outgoing longwave radiation (OLR) and downward surface longwave associated with the temperature basis function a_1
$\epsilon^{\uparrow}_{Rq_1t}$, $\epsilon^{\downarrow}_{Rq_1s}$	-1.0, 1.4 W m^{-2} K^{-1}	Longwave coefficients for OLR and downward surface longwave associated with the moisture basis function b_1
$\epsilon^{\uparrow}_{RT_st}$, $\epsilon^{\downarrow}_{RT_ss}$	0.533, 6.283 W m^{-2} K^{-1}	Longwave coefficients for OLR and upward surface longwave associated with surface temperature variations
$\epsilon^{\uparrow}_{R\alpha_1t}$, $\epsilon^{\downarrow}_{R\alpha_1s}$	70., 18. W m^{-2} K^{-1}	Longwave coefficients for OLR and downward surface longwave associated with cloud type 1 (deep cloud and associated cirrocumulus/ cirrostratus) fraction
$c_{\alpha 1}$	7.76×10^{-4} W^{-1} m^2	Proportionality of cloud type 1 cloud fraction to deep convective heating
$C_p p_T/g$	8.2×10^6 J K^{-1} m^{-2}	Factor to convert longwave T_1 and q_1 coefficients to s^{-1}, or fluxes to K s^{-1}
K_H	3.0×10^5 m^2 s^{-1}	Horizontal diffusion
M_{Sr1}	3.5×10^3 J K g^{-1}	Reference value of the dry static stability component of the gross moist stability
M_{qr1}	3.0×10^3 J K g^{-1}	Reference value of the gross moisture stratification (moisture convergence component of the gross moist stability)
M_{Sp1}	3.4×10^{-2} (unitless)	Change in dry static stability per T_1 change
M_{qp1}	2.7×10^{-2} (unitless)	Change in gross moisture stratification per q_1 change
$p_T = p_{rt} - p_{rs}$	8×10^4 P_a	Reference pressure depth of the troposphere
$r_{s_{min}}$	120 m^{-1} s	Minimum surface resistance for evapotranspiration
W_0	500 mm	Field capacity for soil moisture in tropical forest

obtain total temperature, use $T = T_r(p) + a_1(p)T_1(x, y, t)$ and likewise for moisture. While T_r and q_r are specified, the model produces its own (nonlinear) contributions to the mean stratification. The form of convective heating and moisture sink on the rhs of (5.3) and (5.4) results from the choice $\hat{T}_r = \hat{T}_r^c$, $\hat{q}_r = \hat{q}_r^c$ (see sections 4c, 4d). Effects of the choice of reference profiles are discussed in appendix A.

The contributions to the *advection–diffusion operator* for the momentum equations projected on V_0 and $V_1(p)$, respectively, are given by

$$\mathcal{D}_{V0}(\mathbf{v}_0, \mathbf{v}_1) = \mathbf{v}_0 \cdot \boldsymbol{\nabla}\mathbf{v}_0 + \langle V_1^2\rangle \mathbf{v}_1 \cdot \boldsymbol{\nabla}\mathbf{v}_1 + \langle V_1^2\rangle(\boldsymbol{\nabla} \cdot \mathbf{v}_1)\mathbf{v}_1 - K_H\nabla^2\mathbf{v}_0, \tag{5.11}$$

$$\mathcal{D}_{V1}(\mathbf{v}_0, \mathbf{v}_1) = \mathbf{v}_0 \cdot \boldsymbol{\nabla}\mathbf{v}_1 + \frac{\langle V_1^3\rangle}{\langle V_1^2\rangle}\mathbf{v}_1 \cdot \boldsymbol{\nabla}\mathbf{v}_1 + \mathbf{v}_1 \cdot \boldsymbol{\nabla}\mathbf{v}_0 - (\langle V_1\Omega_1\partial_p V_1\rangle/\langle V_1^2\rangle)(\boldsymbol{\nabla} \cdot \mathbf{v}_1)\mathbf{v}_1 - K_H\nabla^2\mathbf{v}_1, \tag{5.12}$$

where the vertical advection term has been included in both, giving rise to the terms in $(\boldsymbol{\nabla}\cdot\mathbf{v}_1)\mathbf{v}_1$.

The advection–diffusion operators for the temperature and moisture equations (using a vertical average projection) are, respectively,

$$\mathcal{D}_{T1} = \mathbf{v}_0 \cdot \boldsymbol{\nabla} + \hat{a}_1^{-1}\langle a_1 V_1\rangle \mathbf{v}_1 \cdot \boldsymbol{\nabla} - K_H\nabla^2 \quad \text{and} \tag{5.13}$$

$$\mathcal{D}_{q1} = \mathbf{v}_0 \cdot \boldsymbol{\nabla} + \hat{b}_1^{-1}\langle b_1 V_1\rangle \mathbf{v}_1 \cdot \boldsymbol{\nabla} - K_H\nabla^2. \tag{5.14}$$

The terms arising from vertical transfer of momentum to surface stress by parameterized subgrid-scale turbulence, as derived in (4.33)–(4.34), are defined as

$$\begin{aligned}
\epsilon_0 &= (g/p_T)\rho_a C_D \mathrm{V}_s,\\
\epsilon_1 &= \epsilon_1^\tau + \epsilon_1^{\text{int}} = (g/p_T)\rho_a C_D \mathrm{V}_s V_{1s}^2/\langle V_1^2\rangle + g\langle \nu a_1^2 p^{-2}\rangle/\langle V_1^2\rangle,\\
\epsilon_{01} &= (g/p_T)\rho_a C_D \mathrm{V}_s V_{1s}/\langle V_1^2\rangle,\\
\epsilon_{10} &= (g/p_T)\rho_a C_D \mathrm{V}_s V_{1s}.
\end{aligned} \tag{5.15}$$

These are nonlinear functions of model variables due to V_s and potentially other terms. They change according to land surface type through C_D. They have dimensions of inverse timescales but are not equivalent to Rayleigh friction, as discussed in section 7.

Sensible heat and evaporation, using (4.31), (4.30), and (4.32), are given by

$$H = \rho_a C_H V_s (T_s - (T_{rs} + a_{1s} T_1)), \quad (5.16)$$

$$E = \rho_a C_H V_s (q_{\text{sat}}(T_s) - (q_{rs} + b_{1s} q_1)), \quad (5.17)$$

with V_s parameterized according to (A.9), except that evaporation over land regions is given by (6.4)–(6.5). In the numerical implementation, the drag coefficients C_D and C_H follow the Deardorff (1972) formulation, with dependence on surface roughness. Here we use $C_D = C_H$.

Longwave radiation terms are calculated as specified in section 4f, using a weakly nonlinear expansion about precalculated values for T_r and q_r, using a version of the CN96 scheme. Shortwave radiation terms are discussed in ZNC. Table 1 gives values of various parameters and typical values of some variable coefficients; some depend on vertical structures given in ZNC. The values involving b_1 differ from those in ZNC since in that paper b_1 is chosen separately from B_1.

6. Land surface model

As we outline in section 7c, some useful aspects of this approach come from the resulting view of large-scale atmosphere–land interaction. No atmospheric model of the tropical climatology is complete without some specification of land surface processes. Full land models are complex and contain detailed parameterizations for many vegetative types and many detailed processes. Here we outline the approach that we use for a land surface scheme appropriate to this level of model. The most essential features for climate simulation are the low heat capacity of the land surface and the specification of land albedos. The effects of higher roughness over land in bulk formulas, and the effects of varying soil moisture and consequences for evaporation, introduce important subsidiary modifications. Details of land surface–type specifications, and dependence of evaporation on soil moisture, are given in ZNC. The relationship to existing land surface models is discussed there.

We use a single land surface layer with temperature governed by

$$C_s \partial_t T_s = F_s^{\text{net}}, \quad (6.1)$$

where C_s is a land heat capacity; since this is small, on timescales much longer than a day the condition is essentially zero net surface flux:

$$F_s^{\text{net}} \approx 0, \quad (6.2)$$

where

$$F_s^{\text{net}} = S_s^{\downarrow} - S_s^{\uparrow} + R_s^{\downarrow} - R_s^{\uparrow} - E - H. \quad (6.3)$$

Sensible heat flux and surface stress are given by the same bulk formulas as over the ocean, (5.16) and (2.10), except that drag coefficients are higher. They are specified as a function of land surface type as given in ZNC. In section 7, we present results that use a single land value of C_D and C_H to illustrate that for the large scale this is not the leading factor. Surface albedo is specified from observations.

The above relations are fairly standard for simple GCM land representations, and many of the leading land effects are found in the above, including those discussed in section 7c. Much of the complexity of land schemes comes from the representation of evaporation dependence on vegetation and soil moisture. The following representation is motivated by the Biosphere–Atmosphere Transfer Scheme (BATS) (Dickinson 1984; Dickinson et al. 1986) but considerably simplified.

Evaporation over land is modified as

$$E = E_T + E_I, \quad (6.4)$$

where E_I is interception loss, which depends on precipitation. This can be on the order of 25% of the evaporation in the Amazon but less elsewhere. The primary contribution is evapotranspiration:

$$E_T = \rho_a [q_{\text{sat}}(T_s) - q_a](r_a + r_s(W))^{-1}, \quad (6.5)$$

where $r_a = (C_D V_s)^{-1}$ is the aerodynamic resistance. The surface resistance $r_s(W)$ is similar to a combined stomatal and root resistance (Dickinson 1984). It has a minimum value $r_{s_{\min}}$ when soil moisture content W is saturated; r_s increases as the soil moisture drops since plants reduce evaporation when under water stress. Evaporation thus becomes less dependent on wind speed and roughness for low soil moisture, akin to biophysical models. While soil moisture is important to hydrology and land processes, from the point of view of large-scale climate, it is mainly an input to the evaporation calculation, of most relevance in dry conditions.

For interactive soil moisture, we use a single-layer formulation similar to a deep-layer integrated version of BATS:

$$\partial_t W = P - E - R, \quad (6.6)$$

with P the precipitation and R the runoff with surface and ground contributions $R = R_s + R_g$. Surface runoff depends on incoming water flux at the surface ($P - E_I$) and is parameterized as having a strong but smooth increase as the field capacity W_0 is approached. Subsurface runoff R_g increases even more strongly when the soil is near saturation, but it is independent of current precipitation. Details are specified in ZNC.

7. Model properties

a. Form of the equations

An advantage of carrying forward the solution analytically to the form of section 5 is that some properties can be diagnosed directly by inspection of the equations.

1) The most important of these properties is to clarify the effective static stability of the tropical atmosphere, specifically the role of the gross moist stability versus CAPE (see N97 for discussion that includes more on the interpretation of the gross moist

stability). In convective regions, for motions for which τ_c can be assumed small, the thermodynamics is largely governed by (5.6). Thus M_1 acts as the static stability for large-scale motions, giving the amount of energy required to lift a large-scale air mass per unit convergence. The role of conditional instability at the sub-Reynolds scales is reflected in the positive CAPE in the convective heating term in (5.3). Thus small scales can be statically unstable, while large scales evolve with stable stratification. This provides a solution to the mystery of why simple tropical models can use stable stratification in convective regions and obtain plausible solutions.

2) The transition from convective to nonconvective regions occurs when projected CAPE drops below zero and convection is no longer supported (see section 4d for discussion of this measure of CAPE). In nonconvecting zones, the temperature equation (5.3) takes over as the important thermodynamic equation. The moisture equation is partially decoupled from the dynamics and responds passively to circulation (except as it affects the radiation field and the $\mathbf{v}\cdot\nabla q$ term at the edge of convection zones). Thus in nonconvecting zones, the dry static stability M_{s1} applies, and the transition from convecting to nonconvecting regions is primarily a change in effective stability of the motions. This helps justify the assumption used in some simple models (e.g., Zebiak 1986) that convective regions simply have a reduced stability. It also provides a more rigorous alternative to such assumptions: the surface flux forcing terms linking the thermodynamics to SST change as (5.3) takes over from (5.6), as does the effective heat capacity, which in (5.6) includes effects of moisture.
3) The transition from convective to nonconvective regions is traditionally thought of as highly nonlinear because convective heating goes from positive values to zero. However, from the point of view of temperature, the transition from being governed by (5.6) to being governed by (5.3) is a relatively gentle one, allowing the temperature field to be continuous and smooth. Even if heating were to flicker on and off, temperature would tend to integrate over these variations. Thus linearization of these equations to produce simplified models can be productive.
4) Although the model is set up to be most accurate in situations near QE, departures from QE are permitted within convective regions, and these can produce substantial effects, especially at small scales. A relevant scaling (even for steady motions) is the comparison of a timescale associated with dry gravity wave adjustment (length scale over phase speed) versus the convective adjustment timescale (see N97). At smaller scales these effects become competitive, and this tends to produce a damping effect on perturbations. To the extent that motions evolve in QE, the strong damping on CAPE seen in the moisture and temperature equations (5.3)–(5.4) individually is irrelevant. To the extent that motions depart from QE, this damping is exerted on the parts of the solution tending to produce CAPE. We also note that the strict QE limit [which in the case of (5.5) is $q_1 \approx T_1$] does not imply that the convective heating is small since it only applies when ϵ_c^* is large. Departures from QE can always be calculated even when using the QE approximation to simplify analysis. The model can thus be used to critically examine the QE approximation. It may thus be useful in assessing why, for instance, Brown and Bretherton (1997) find a relationship between observed upper-level temperature and boundary layer moist enthalpy that is qualitatively consistent with QE predictions at some scales, but with a smaller proportionality coefficient than would be predicted by strict QE assumptions.
5) The terms arising from vertical transfer of momentum onto surface stress, with coefficients given by (5.15), have parameters, such as the drag coefficient and the vertical viscosity, that are directly comparable to those used in GCMs. Although they help explain why simple models could use Rayleigh friction for some aspects of the tropical problem, they also show how a more systematic solution differs from this. The coefficients ϵ_0 and ϵ_1 do act like spindown rates for the barotropic and baroclinic components of the wind, respectively. However, the terms with ϵ_{01} and ϵ_{10} act as a transfer between these two components. Differential heating drives the baroclinic component of the wind, but as surface drag opposes this component, it tends to spin up a barotropic component of the wind. The barotropic component is less strongly damped, so a local heat source can produce a nearly barotropic response in the far field. The surface drag tends to produce a barotropic component that opposes the baroclinic component near the surface and thus reinforces it aloft, resulting in a tendency to weaker surface winds and stronger upper-level winds. Of course, the barotropic component cannot exactly cancel the surface wind pattern since the nonlocal dynamics of both components has different characteristic length scales.
6) The difference between simple model damping and the QTCM terms becomes particularly clear when considering equations governing the zonally averaged flow. Specifically, if we consider the zonal momentum equation (2.4) from the primitive equations, vertically integrating and taking the zonal mean, we have

$$\partial_t[\hat{u}] + [\widehat{\mathbf{v}\cdot\nabla u}] + [\widehat{\omega\partial_p u}] - K_H\partial_y^2[\hat{u}] = -(g/p_T)\tau_s^x, \tag{7.1}$$

where [ ] denotes zonal averaging and we have used $[\hat{v}] = 0$. In the time average, where the time derivative term may be neglected, the surface stress at the equator is balanced by nonlinear terms (the contribution of horizontal diffusion is small). These pri-

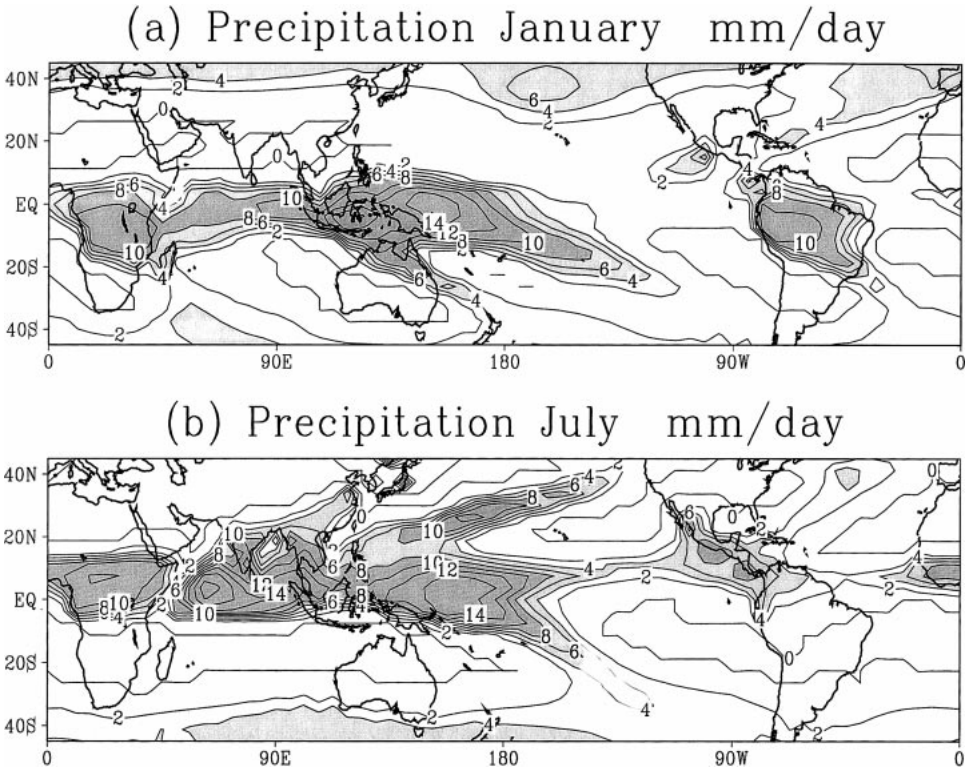

FIG. 2. Simulated climatology of precipitation (averaged 1982–91) for (a) Jan, (b) Jul. Contour interval 2 mm day^{-1}, shading and heavy shading over 4 and 8 mm day^{-1}. The region shown is a subset of the model domain, which extends to 60° latitude.

marily consist of transient eddy transports. Without nonlinear advection terms, the surface wind stress must be tiny everywhere. The same balances are reflected in the QTCM, unlike models that use Rayleigh friction. For a model with Rayleigh friction, the damping term on the rhs of (7.1) would be $\epsilon_{\text{Rayleigh}}\,[\hat{u}]$, so the baroclinic wind would not be constrained as it should be by (7.1). In the QTCM, as in the primitive equations, momentum is transported by advection, and damping occurs by vertical transport down to the surface.

b. Examples of climatological simulation

Model behavior is be discussed in detail in ZNC, but a brief example of the simulation of the tropical climatology aids concrete discussion of the model properties. We present here the climatological January and July simulations, calculated as the average over an integration with time-varying observed SST (Reynolds 1988) from 1982 to 1991. Topography is not included. The version presented here differs from the main case in ZNC in that it includes cloud feedbacks only for deep and CsCc clouds, the simpler of the two radiation schemes is used, and the choices in parameters that lead to the simplest form of the convective heating (5.5) are used. Since the latter have only small effects, the case here may be approximately compared to the corresponding case in ZNC, but with the land surface simplified to use a single drag coefficient and field capacity. This corresponds to having a single land surface type (here, forest), except that albedo is specified as a function of space and season. This serves to illustrate that for global climate, detailed specification of land surface properties is a second-order effect (although locally, it can be important). Albedo variations in space must be included to get a suitable representation of land summer rainfall (seasonal variations are a next-order effect but are included for consistency with ZNC).

The climatological precipitation pattern (Fig. 2) can be compared quantitatively to observations, which may be considered good performance for a model of intermediate complexity simulating the full climatology. In January, the South Pacific Convergence Zone is well simulated, as is the western Pacific region and the extension across the Indian Ocean. The Pacific ITCZ north of the equator is too weak in the east compared to the Xie and Arkin (1996) satellite/gauge estimate. In July the precipitation in the western Pacific is relatively strong near the date line and relatively weak over Indonesia. This is associated with the evaporation–wind feedback favoring convection in the region where strong trade winds meet the warm pool. The ITCZ in the Atlantic is slightly weak compared to the continental re-

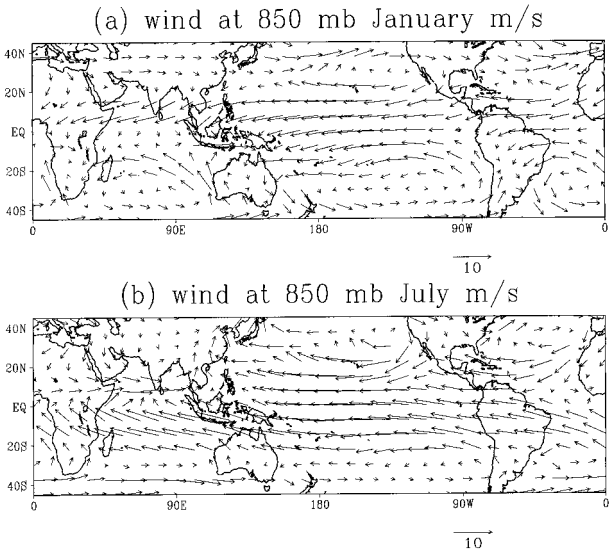

FIG. 3. Simulated climatology of 850-mb wind field (m s^{-1}) for (a) Jan and (b) Jul.

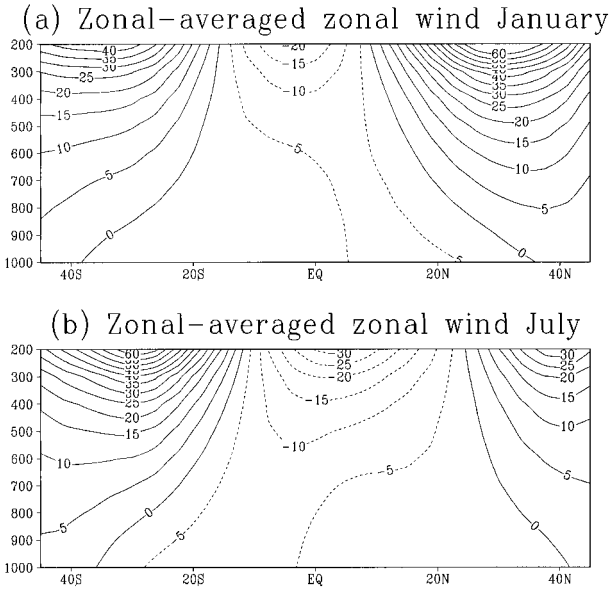

FIG. 4. Simulated climatology of the zonal-mean zonal wind as a function of latitude and pressure for (a) Jan and (b) Jul. Contour interval 5 m s^{-1}.

gions but has the correct spatial form. The eastern Pacific dry zone and its extension westward along the equator are simulated.

The pattern of dry desert regions and monsoon convection regions over continents is affected by the interactive soil moisture; its simulation and impact will be discussed in ZNC. The convergence zones over land depend on consistent modeling of both radiative terms and land surface interactions. Since SST is specified, any error (or uncertainty) in the surface solar radiation, or the cloud feedbacks affecting this, will tend to show up in the land convergence zones, providing a significant test of the physics package. While the African convergence zone is slightly too broad, its position and seasonal shifts are reasonable. The South American convergence zone is quite well simulated in southern summer. There is even a representation of the dry notch over the Nordest region of Brazil, although such regional features are sensitive to model parameters. In northern summer, the convection moves up into the Mexican monsoon region. We note that this model version does not include the trade inversion, but apparently a representation of deep convection and compensating deep descent can capture many features of the tropical climatology.

The midlatitude storm tracks are shifted slightly poleward of the observed but have qualitatively reasonable latitude and magnitude, although individual storms are slightly too strong in this model. The storm track precipitation is shifted eastward compared to observations in both the Atlantic and Pacific in this version. Using the moisture closure (2.22) instead of (2.23) has significant impact on these features (H. Su 1999, personal communication). Since the moisture field is consistently simulated in this model, obtaining the subtropical dry zones and desert regions depends importantly on the subtropical moisture fluxes by midlatitude baroclinic eddies. It is pleasing that the model performs plausibly in this, since the approximations were set up to be optimal in the Tropics but appear to work acceptably at the midlatitude edges of the domain.

The pattern of 850-mb winds (Fig. 3) compares well with the National Centers for Environmental Prediction analysis (not shown). The region of westerlies north of Australia is approximately correct, and the central and east Pacific trades are good, including significant meridional component in the east, something that is difficult to simulate in simple models. This is obtained despite not yet including a separate basis function for boundary layer modifications to the baroclinic wind field. Turning occurs here because we have treated vertical momentum transport in a manner consistent with the primitive equations: momentum loss is by transfer to surface stress, instead of using a Rayleigh friction where momentum simply disappears from the interior of the atmosphere. As a result, the surface drag tends to reduce surface wind by partial cancellation of the baroclinic and barotropic components, whereas they reinforce each other aloft to produce subtropical jet streams.

The subtropical jets may be seen in the latitude pressure cross section (Fig. 4) of zonal mean zonal wind. Although there are only two vertical degrees of freedom in the numerical solution, the effort expended on analytical vertical solution gives more realistic vertical structures than would finite differencing with the same degrees of freedom. The reduction in speed of the jet above the tropopause cannot be captured, of course,

since there is no stratosphere in which to reverse meridional temperature gradients. The transition to surface westerlies occurs a bit too far poleward in the summer hemisphere. However, recalling (section 7a) that the QTCM obeys the same integral constraints as the primitive equations (7.1), the zonal average surface stress depends on correctly modeling nonlinear momentum transports, especially those associated with transient eddies. Considering this, the reasonable simulation of tropical surface easterlies is quite satisfactory.

c. Some simple consequences for land–atmosphere interaction

The form of the model, combined with the surface heat flux balance condition (6.2), helps simplify understanding of land–atmosphere interactions at large scales. Here only the most basic consequences of (6.2) are outlined. A detailed example for the case of Amazon deforestation, including consequences of soil moisture effects and cloud–radiative feedbacks is presented in Zeng and Neelin (1999) using a simple model derived from these considerations.

The moist static energy equation (5.6) with (6.2) becomes

$$\hat{a}_1(\partial_t + \mathcal{D}_{T1})T_1 + \hat{b}_1(\partial_t + \mathcal{D}_{q1})q_1 + M_1\boldsymbol{\nabla}\cdot\mathbf{v}_1 = (g/p_T)F_t^{\text{net}} = (g/p_T)(S_t^{\downarrow} - S_t^{\uparrow} - R_t^{\uparrow}). \quad (7.2)$$

This view immediately makes clear that top-of-the-atmosphere balances are crucial to the atmosphere–land system in convecting regions. While land processes may affect the partition of the land surface energy budget, the net transfer of energy between the surface and the atmospheric column remains zero. Diagnostics based on the moist static energy budget thus have an attractive simplicity, especially over land, in convective regions. Under convective conditions, to a first approximation, the moist static energy budget makes land–atmosphere interactions appear in some ways simpler than the corresponding ocean–atmosphere interactions. Since the outgoing longwave radiation $R_t^{\uparrow}$ depends strongly on the atmospheric state, as does the reflected upward shortwave at the top of the atmosphere $S_t^{\uparrow}$, the downward solar input $S_t^{\downarrow}$ is clearly identified as the fundamental forcing of the system. However, because cloud albedo feedbacks and cloud dependence of OLR can modify F_t^{net} quite significantly, this view also highlights the importance of cloud feedbacks. In considering interannual anomalies, assuming that one remains in a convecting region, any anomalies in convergence must be balanced either by advection terms $[(\mathcal{D}_{T1}T_1 + \mathcal{D}_{q1})q_1)$ from $\mathbf{v}\cdot\boldsymbol{\nabla}(T + q)]$ or by anomalies in $S_t^{\uparrow} + R_t^{\uparrow}$.

We also note that over ocean, atmospheric anomalies that are excited remotely can experience thermodynamic damping by loss of heat into the ocean surface. Heating in one region tends to produce warm temperatures in adjacent regions, but these are gradually damped by anomalous losses of sensible and latent heat and anomalous longwave radiation down to the surface as well as up to space. Over land, on the other hand, any components of the heat budget that go into the surface must be balanced in one way or the other by opposing changes in other surface heat budget terms. The atmosphere can only experience thermodynamic damping by radiative losses to space. Thus atmospheric teleconnections will tend to have longer characteristic teleconnection distances over land than over ocean.

Many of these properties will be exploited in ongoing work on specific examples of atmosphere–land interaction. Discussion of the effects of soil moisture is deferred to that work. Similar budgetary considerations apply in GCMs. From the intermediate model it simply becomes clear that the moist static energy budget governs the thermodynamics of convective regions when certain approximations are met. Specifically, when deep convection constrains temperature through the depth of the troposphere, and connects dry and moist thermodynamics, then the partition of the surface energy fluxes becomes secondary to the net flux. These conditions are met in QE but may be useful as a starting point even in a GCM under non-QE conditions.

d. Model simplifications for diagnostic purposes

Further approximations can be made to the QTCM equations to produce simple models aimed at understanding specific phenomena. We list some examples here, along with some properties that may be exploited in further work or by other investigators.

1) The steady solution to these equations is well posed and can be a reasonable approximation to the full solution in the Tropics under some circumstances. The tropical solution is well posed as a steady solution because of the positive gross moist stability in convecting regions, as discussed in section 7a. The presence of positive CAPE in some regions leads to a well-defined mean convective heating in those regions, even without transient effects at the large scale. We have tested steady solvers for versions of the model, using multigrid methods, and obtained reasonable solutions for idealized cases. For the particular implementation tested, we did not obtain sufficient increase of solution speed compared to time integration to justify the added code complexity. However, in principle a steady solution version could be fruitful for study of climate anomalies, such as ENSO response. Omission of (or necessity of approximating) midlatitude transient eddy transports is the leading effect with consequences for the climatology, as discussed below. Soil moisture is not well approximated by steady solutions over the seasonal cycle.
2) Midlatitude eddies can be ''turned off'' using approximations to the $\mathbf{v}\cdot\boldsymbol{\nabla}T$ term, $\mathcal{D}_{T1}T$ in (5.3), since

temperature advection is the fundamental energy source for baroclinic instability. This is used in Lin et al. (1999) to test the effects of midlatitude eddies on tropical intraseasonal variability. In Lin et al., the $\mathcal{D}_{T1}T$ is simply replaced by its climatological value from a control run. Midlatitude storms disappear, but the climatological heat transport is maintained. A more gentle approach (not yet implemented) would be to approximate all advection terms by running averages during time integration and to specify transient eddy statistics from a control run. If midlatitude transient eddy effects are entirely omitted, excess rainfall tends to occur in the subtropics in the climatological solution, often appearing as a broadening or extension of the ITCZs, due to the lack of dry static energy and moisture transports from the subtropics to midlatitudes. Some simple models have sidestepped this problem in the past by specifying low-level moisture, thus downplaying the role of transients. It seems more consistent to specify eddy transports and simulate moisture.

3) For simplified studies, solutions can be obtained omitting all the $\mathbf{v}\cdot\nabla$ advection terms, as has been traditional in simple tropical models. However, the effect of these terms is often not as small as the simplest scaling arguments would suggest. Besides the lack of baroclinic eddy transports, moisture and temperature advection can be important to wave phenomena and hence to teleconnection phenomena within the Tropics. To estimate their effects in convecting regions, they should be compared to moist static energy divergence, rather than to the larger but canceling dry static energy divergence and moisture convergence. Rather than omit $\mathbf{v}\cdot\nabla$ terms, for some problems they can be better approximated by linearization about a mean wind. However, as noted in Zeng (1998) and Zeng and Neelin (1999), when these terms are omitted, the solution for the convergent motions can be reduced to an effectively local thermodynamic problem.
4) Within deep convective regions, for large timescales and space scales, the thermodynamics may be approximated by the moist static energy equation with $q_1 \approx T_1$, as occurs when ϵ_c^* may be assumed large. CAPE and precipitation may be diagnosed after solution.
5) Useful simplifications can be obtained by fixing M to a climatological or constant value for analysis of basic dynamics in deep convective regions, as in point 4. However, in descent regions, allowing M_q to vary is important to establishing balance by reduction of the moisture that is diverged.
6) Over land, solutions with the diurnal cycle omitted may differ quantitatively but tend to be qualitatively similar for many problems. For problems that do not require solution of the seasonal cycle of climatological precipitation, or variability associated with soil moisture, the soil moisture equation may be omitted and a single value of the surface resistance substituted. Even for simulation of annual mean climatology, when albedo is specified, an acceptable climatology can be obtained using a fixed value of r_s.
7) Although for the total wind field it is seldom a good approximation, for many of the thermodynamic fields and the baroclinic wind convergence it can sometimes be acceptable to neglect $\epsilon_{01}\mathbf{v}_0$ in (5.1). Then if baroclinic advection terms are small, the baroclinic component solution decouples from the barotropic solution, so a baroclinic mode solution can be studied, akin to simpler models.
8) Linearization can hold reasonably well for many problems, as discussed in section 7a, point 3. Exceptions include shifts of the edge of the tropical convergence zones, which can be important in some interannual climate anomalies.

8. Summary and discussion

We have presented here a nonlinear tropical circulation model that represents tropical dynamics using a formulation that begins from the interaction of the ensemble effects of convection with the large-scale circulation, rather than formulating a model for conventional ''dry'' dynamics and then considering how it might interact with convection. The model makes use of constraints from a particular QE convective scheme, the Betts–Miller scheme, but does not assume that convective QE has to hold. N97 outlined results of a project based on examining implications of QE constraints for the large-scale tropical flow. Here we present the simplest model that works through these implications, while not being strictly bound by QE assumptions. Using a combination of analytical and numerical approaches, the model takes analytical solutions that hold approximately under QE conditions and employs them as leading basis functions to represent the vertical structure of the flow. In conditions where convective QE holds well, the model is designed to be accurate with very few vertical degrees of freedom. Outside convective regions, it is simply a model with a highly truncated Galerkin representation in the vertical. We recognize that the case presented here, with a single vertical basis function in temperature (two in velocity), will not perfectly capture all tropical phenomena. However, it is of interest to push this simplest version as far as possible, given the considerable success that it appears to show.

The model is computationally very economical, essentially because part of the solution has been carried out analytically before turning to the numerics. However, we argue that the main advantage that the model offers, under suitable conditions, is a relative simplicity of analysis. For many tropical phenomena, especially those involving the ensemble average effects of deep convection, relatively few vertical degrees of freedom participate. To the extent that the derivation used here

is appropriate to those phenomena, it is easier to analyze this QTCM than most other models, including some ''simple models.'' This provides motivation for shoehorning as much physics as possible into the heavily truncated Galerkin framework (using other approximation techniques to extend the ordinary Galerkin approach where necessary). By including treatment of radiative processes, cloud radiative interactions, and land surface processes, and by maintaining parameters and parameterizations that are as consistent as possible with corresponding representations of these processes in GCMs, we obtain a system that can complement GCMs for a fairly wide class of problems, but which admits of further simplifications for analysis.

The role of the moist static energy budget aids considerably in the analysis of dynamics of convective regions in this model. In convective regions, the moist static energy budget avoids the large and canceling terms due to convective heating and moisture sink that tend to distract attention from the more subtle balances driving tropical flow. In strict QE conditions in deep convective regions, the moist static energy equation governs the thermodynamics of the flow since convection ties together moisture and temperature equations and links temperature through the troposphere with boundary layer moist static energy. As a result of these contraints, there is a gross moist stability M (NY94; YCN) that gives the net static stability for large-scale motions including the partial cancellation of adiabatic cooling by convective heating. This allows direct examination of the balance between convergent motions and the net flux of heat into the atmospheric column. Over land, in convective regions, this balance becomes particularly useful since the net surface heat flux must sum to zero. This highlights the importance of consistent treatment of vertical energy fluxes over land regions and makes this model particularly amenable to simplifications for analysis of land regions (e.g., Zeng and Neelin 1999).

At the same time as having a well-defined static stability for large scales, the model convection is driven by a measure of CAPE that indicates the degree of conditional instability at the subgrid scale. Although the model is set up to be most accurate if convective QE holds well, it does permit the possibility of critically examining at least some of the QE assumptions. We picture QE as holding best at large timescales and space scales; at sufficiently small scales, QE must necessarily fail for lack of an adequate number of convective elements in the ensemble. We hope that this model will aid in quantifying the crossover point between scales where QE is a powerful tool for examining tropical flow and scales where the motions that consume CAPE come into play. Throughout our derivation, we have tried to point the way to places where assumptions can be relaxed while still maintaining the advantages of the approach. Likewise, we have tried to indicate ways that the model can be simplified for theoretical studies.

Finally, we provide an example of model performance when challenged with the simulation of the tropical climatology. Although we defer fuller examination of the simulation to subsequent work (ZNC), the reproduction of certain tropical climate features is comparable to that of many GCM studies. This serves to illustrate concretely that this system can provide useful simulations not only for climate anomalies but for many aspects of the full tropical climate. This simulation also helps remind us of caveats to the notion of modeling the Tropics with special approximations since transient motions associated with midlatitude baroclinic eddies do affect the subtropical solution and hence the Tropics. Fortunately, although the model approximations are aimed at tropical convective regions, it also holds adequately as midlatitudes are approached that it may be possible to investigate some aspects of midlatitude–tropical interactions [see Lin et al. (2000) for an example with intraseasonal variability]. This climatological simulation also provides an indication that the interactive land surface scheme works reasonably well in conjunction with this model.

It is hoped that the model presented here will fill a useful niche in the arsenal of tools available for tropical problems. The numerical implementation of the model is available to interested colleagues.

Acknowledgments. This work was supported in part by National Science Foundation Grant ATM-9521389 and National Oceanographic and Atmospheric Administration Grant NA86-GP0314. Early stages of this work were carried out while the authors were visiting the Massachusetts Institute of Technology Department of Earth, Atmospheric, and Planetary Sciences; JDN acknowledges support from the Houghton Lectureship. Conversations with A. Arakawa, C. Bretherton, H. Dijkstra, K. Emanuel, A. Kasahara, A. Majda, R. Seager, M. Yanai, and S. Zebiak were helpful. Thanks are due to other group members who have been involved in this project or contributed comments: A. Adcroft, C. Cassou, J. Lin, W. Weibel, J.-Y. Yu, and especially C. Chou and H. Su.

APPENDIX A

Notes to the Derivations

a. Geopotential (see section 4a)

To reconstruct total geopotential at any level from the projected solutions,

$$\phi = \phi_{s0} + \phi_{s1} + a_1^+(p)\kappa T_1, \qquad \text{(A1)}$$

where ϕ_{s1} is given by (4.11). Since ϕ_{s0} is not needed in the solution using (4.12), it can be diagnosed postsolution using the divergence equation derived from (4.6).

b. Regarding projection of T and q equations (see section 4c)

When more basis functions are included in the temperature and moisture equations, a series of test functions $\tilde{a}_k$, $\tilde{b}_k$ must be defined [Petrov–Galerkin technique, e.g., Hirsch (1988)] to multiply the temperature and moisture equation by before taking the vertical average. Here we have simply set the first test function to a constant. Since a_1 and b_1 are of a single sign, an example extending the series while retaining the same a_1, b_1 and retaining the properties of the leading equation would be $\tilde{a}_k = a_1^{-1}a_k$, which would correspond to a conventional choice of $\tilde{a}_k = a_k$ with an inner product weighted by a_1^{-1}. In practice, it is easier to treat, for example, the PBL separately, corresponding to test functions that are unity in the PBL and zero above, and vice versa.

c. Moisture basis function permitting spatial variations (see section 4d)

If the moisture basis function b_1 has spatial variations, the advection operator is modified from (5.14) as

$$\mathcal{D}_{q1} = \mathcal{D}_{q1|(5.14)} + \hat{b}_1^{-1}\,(\mathbf{v}_0\cdot\boldsymbol{\nabla}\tilde{b}_1 + \mathbf{v}_1\cdot\boldsymbol{\nabla}\langle V_1 b_1\rangle) \quad \text{(A2)}$$

(other quantities, such as p_{rs}, V_1 remaining spatially constant). This is only useful computationally if b_1 variations are limited, but it could allow greater freedom, for instance, in treating descent zones with a basis function chosen differently than that chosen here for convective zones, or in modifying b_1 as midlatitudes are approached. There is also a class of variations of b_1 that leave $\hat{b}_1$ and $\langle V_1 b_1\rangle$ approximately constant while modifying M_{q1} and b_{1s}, which is important to evaporation.

d. Low-moisture cases (see section 4d)

As moisture becomes low in desert regions or higher latitudes, it is necessary to ensure that the representation chosen for the Tropics does not create spurious negative moisture effects, in particular that $M_{q1} > 0$ and $q_{rs} + b_{1s}q_1 > 0$. In a descent region ($\boldsymbol{\nabla}\cdot\mathbf{v}_1 < 0$), if no source terms are present, moisture tends to decrease exponentially by low-level divergence toward $M_{q1} = 0$. If surface moisture reaches zero first, we simply modify b_1 in those regions such that it does not drop below zero. If (3.13) is used, this is not needed. Caution must be used in applying (2.23) in regions with very cold temperatures (e.g., high-latitude land in winter), as it may drive moisture toward negative values; switching to (2.22) solves this.

e. Effects of changing reference profiles

The convective reference profiles T_r^c, q_r^c appear only in the convective heating and moisture sink terms, and in this model disappear when the choice $\hat{T}_r = \hat{T}_r^c$, $\hat{q}_r = \hat{q}_r^c$ is made. The reference profiles T_r, q_r appear explicitly only in terms without horizontal or time differentiation: the vertical stratification terms M_{Sr1} and M_{qr1} and the fluxes E and H (which are affected only by surface values). They appear implicitly in several coefficients, due to derivatives evaluated at the reference profiles. Specifically, (i) a_1, and thus V_1, depend on $T_r^c(p_s) + q_r^c(p_s)$ through the moist adiabat; (ii) for the choice $B_1 = [\alpha dq_{sat}/dT]_{T_r^c}$, B_1 has the same dependence as (i); and (iii) the coefficients in longwave radiation depend on both q_r and T_r. In general, these implicit effects via the coefficients are small for modest changes in tropical reference profile.

In principle, the model should be insensitive to explicit effects of certain types of changes in reference profiles. Neglecting the implicit changes via the coefficients, the physics of the model solution is approximately invariant under small changes:

$$T_r \to T_r + a_1(p)\delta T_{r1}, \qquad q_r \to q_r + b_1(p)\delta q_{r1}, \quad \text{(A3)}$$

where δT_{r1} and δq_{r1} are scalars. This is because it can be compensated in M_{S1}, M_{q1}, H, and E by

$$T_1 \to T_1 - \delta T_{r1}, \qquad q_1 \to q_1 - \delta q_{r1}. \quad \text{(A4)}$$

This shift also compensates in $\langle Q_c\rangle$ and $\langle Q_q\rangle$ when T_r and q_r appear explicitly, as in (4.25). When one sets $\widehat{T_r} = \widehat{T_r^c}$, $\widehat{q_r} = \widehat{q_r^c}$, the reference terms do not appear in (5.5), but the shift (A4) still holds because

$$\delta q_r^c \approx B_1 \delta T_r^c \quad \text{(A5)}$$

since small changes in the convective reference profiles must obey (2.23). Applying $\delta\widehat{T_r} = \delta\widehat{T_r^c}$, $\delta\widehat{q_r} = \delta\widehat{q_r^c}$, this implies

$$\delta T_{r1} = (\hat{b}_1/\hat{B}_1)\delta q_{r1}, \quad \text{(A6)}$$

so in the heating term (4.25), the changes also compensate. Thus when using the form of the heating in (5.5), it is important that the T_r^c and q_r^c terms are suitably linked. In practice, this approximate invariance is affected by nonlinearities in M_s and M_q, especially for cold, dry situations.

f. Bulk formula wind speed dependence (see section 4e)

In the model version here, we do not include an explicit representation of the boundary layer winds, but we can parameterize the reduction in wind speed at the surface as it appears in V_s. A simple parameterization is

$$V_s = (V_{s_{min}}^2 + |\eta\mathbf{v}(p_b)|^2)^{1/2}, \quad \text{(A7)}$$

where $V_{s_{min}}$ is a constant representing effects of sub-Reynolds wind variations, and $\eta \le 1$ parameterizes the surface wind speed as proportional to the large-scale wind speed at a level closer to the top of the boundary layer, p_b. Typically, we use $\eta = 0.7$, $V_{s_{min}} = 5$ m s^{-1}, and $p_b = 900$ mb, as discussed in ZNC. More sophisticated approximations to boundary layer wind reduction in the remainder solutions are also possible.

g. Topography via ω_s

Using boundary condition (2.7), it is straightforward to add an approximation to topography that neglects p_s variations in vertical integrals and in vertical structures and that approximates lifting as nonzero ω_s at p_{rs}. The continuity equation then produces nonzero $\boldsymbol{\nabla}\cdot\mathbf{v}_0$ and associated vertical velocity ω_0, replacing (4.5) by (4.4) and using (4.2). A main effect is a barotropic Rossby wave source from $\boldsymbol{\nabla}\cdot\mathbf{v}_0$ using (4.12) instead of (5.2). The divergent wind contribution to $\mathbf{v}_0$ can be computed from $\boldsymbol{\nabla}\cdot\mathbf{v}_0$, although it tends to be small. Adiabatic cooling and moistening effects occur by adding terms $M_{S0}\boldsymbol{\nabla}\cdot\mathbf{v}_0$ and $M_{q0}\boldsymbol{\nabla}\cdot\mathbf{v}_0$ to (5.3) and (5.4), respectively, where $M_{S0} = p_T^{-1}\int_{p_{rt}}^{p_{rs}} \Omega_0\,(-\partial_p s)\,dp$ and $M_{q0} = p_T^{-1}\int_{p_{rt}}^{p_{rs}} \Omega_0\partial_p q\,dp$, with Ω_0 from (4.2). This is an admittedly imperfect representation of topographic effects since changes in atmospheric pressure depth are not small, and since it does not include rainfall by low-level saturation during forced uplift. There is also sensitivity to the wind level used in estimating ω_s, as occurs also in more complex models. The separation of barotopic Rossby wave and baroclinic forcing terms can be useful for analysis purposes.

APPENDIX B

Vertical Structure of Convective Heating Using Remainder Equations

To illustrate approximate solution of remainder equations (see section 3c) with an important case, consider truncation $K = 1$ in (B1) applied in the temperature equation (2.1), focusing on the time derivative and adiabatic cooling terms to illustrate normal terms, and the convective heating term to illustrate a term where the remainder solutions may gainfully be examined. In a convective region, using (2.17) and (2.18) with (3.14) and similar expansions for other terms, (2.1) becomes

$$\partial_t(a_1(p)T_1 + T_R) + (\omega_1 + \omega_R)\partial_p(s_r + s_1T_1 + s_R) + \cdots = (a_1(p)T_1^c - a_1(p)T_1 - T_R)\tau_c^{-1}. \quad \text{(B1)}$$

The term on the rhs is Q_c; ω_R and s_R denote residual components of the solution for vertical velocity and dry static energy (see section 4c), while the retained components, ω_1 and s_1, are given by (4.1) and (4.19). For simplicity, $T_r = T_r^c$ has been used, but inclusion is straightforward. Upon projection (section 4c), (B1) yields the T_1 equation (5.3), solved as part of the model system. However, because τ_c^{-1} is large, the solution for the heating vertical structure would be very poor if only $a_1(p)$ terms were retained. The projected equations give only the vertical average of Q_c. NY94 showed that expanding in orders of τ_c gives a QE solution $T_1 = T_1^c$ at leading order and that the temperature equation simply becomes diagnostic for the heating vertical structure at next order. Likewise here, once T_1 has been obtained, (B1) can be used: on the lhs, T_R and similar terms are neglected, but on the rhs, T_R is multiplied by a large number and so is retained, yielding the solution for T_R and, more importantly, of Q_c. This gives a more detailed vertical structure for Q_c from the resolved terms of the lhs:

$$\begin{aligned} Q_c(x, y, p, t) = {} & a_1(p)\partial_t T_1(x, y, t) \\ & + a_1(p)(\mathbf{v}_0 + V_1(p)\mathbf{v}_1)\cdot\boldsymbol{\nabla}T_1 \\ & + \Omega_1(p)\boldsymbol{\nabla}\cdot\mathbf{v}_1(x, y, t)\partial_p(s_r(p) + s_1(p)T_1) \\ & - Q_R - g\partial_p F_T. \end{aligned} \quad \text{(B2)}$$

The radiative heating $Q_R = g\partial_p R^{\uparrow} - g\partial_p R^{\downarrow} - g\partial_p S$ as a function of height can be obtained from expressions equivalent to (4.35) but evaluated at additional levels in the linearized longwave scheme for T_1, q_1 and cloudiness values (to include vertical structure of solar absorption, a similar procedure could in principal be followed—currently only column average absorption is used). Sensible heat flux is distributed in some reasonable way over the PBL.

This approximate solution for the vertical structure of the heating can change continuously with the model solution, despite having only a single temperature basis function, since the vertical structures of, for example, the temperature–time derivative term and the adiabatic cooling term, are different. The heating thus can have different vertical structure for rapidly time varying phenomena and slow phenomena. As shown in NY94 and Yu and Neelin (1994), this solution for the heating can look quite realistic even for simplified model versions, and it is very different than what would be obtained from the $a_1(p)$ terms alone. This structure is not required in the solution method but can be diagnosed.

REFERENCES

Arakawa, A., 1993: Closure assumptions in the cumulus parameterization problem. *The Representation of Cumulus Convection in Numerical Models of the Atmosphere, Meteor. Monogr.*, No. 46, Amer. Meteor. Soc., 1–15.

——, and W. H. Schubert, 1974: Interaction of a cumulus cloud ensemble with the large-scale environment. Part I. *J. Atmos. Sci.*, **31,** 674–701.

Betts, A. K., 1986: A new convective adjustment scheme. Part I: Observational and theoretical basis. *Quart. J. Roy. Meteor. Soc.*, **112,** 677–691.

——, and M. J. Miller, 1986: A new convective adjustment scheme. Part II: Single column tests using GATE wave, BOMEX, ATEX and arctic air-mass data sets. *Quart. J. Roy. Meteor. Soc.*, **112,** 693–709.

——, and ——, 1993: The Betts–Miller scheme. *The Representation of Cumulus Convection in Numerical Models, Meteor. Monogr.*, No. 46, Amer. Meteor. Soc., 107–121.

Bladé, I., and D. L. Hartmann, 1993: Tropical intraseasonal oscillations in a simple nonlinear model. *J. Atmos. Sci.*, **50,** 2922–2939.

Brown, R. G., and C. S. Bretherton, 1997: A test of the strict quasi-equilibrium theory on long time and space scales. *J. Atmos. Sci.*, **54,** 624–638.

Chou, C., 1997: Simplified radiation and convection treatments for large-scale tropical atmospheric modeling. Ph.D. dissertation,

University of California, Los Angeles, Los Angeles, CA, 215 pp. [Available from Department of Atmospheric Sciences, UCLA, Box 951565, Los Angeles, CA 90095-1565.]

——, and J. D. Neelin, 1996: Linearization of a long-wave radiation scheme for intermediate tropical atmospheric models. *J. Geophys. Res.,* **101,** 15 129–15 145.

Crum, F. X., and D. E. Stevens, 1983: A comparison of two cumulus parameterization schemes in a linear model of wave-CISK. *J. Atmos. Sci.,* **40,** 2671–2688.

Deardorff, J. W., 1972: Parameterization of the planetary boundary layer for use in general circulation models. *Mon. Wea. Rev.,* **100,** 93–96.

Dickinson, R. E., 1984: Modeling evapo-transpiration for three-dimensional global climate models. *Climate Processes and Climate Sensitivity, Geophys Monogr.,* No. 29, Maurice Ewing Volume 5, Amer. Geophys. Union, 58–72.

——, A. Henderson-Sellers, P. J. Kennedy, and M. Wilson, 1986: Biosphere–Atmosphere Transfer Scheme (BATS) for the NCAR Community Climate Model. NCAR Tech. Note TN-275+STR, NCAR, Boulder, CO, 69 pp.

Emanuel, K. A., 1994: *Atmospheric Convection.* Oxford University Press, 580 pp.

——, 1998: Quasi-equilibrium thinking. *General Circulation Modeling: Past, Present, and Future,* D. A. Randall, Ed., Academic Press, in press.

——, J. D. Neelin, and C. S. Bretherton, 1994: On large-scale circulations in convecting atmospheres. *Quart. J. Roy. Meteor. Soc.,* **120,** 1111–1143.

Gill, A. E., 1980: Some simple solutions for heat induced tropical circulation. *Quart. J. Roy. Meteor. Soc.,* **106,** 447–462.

Guckenheimer, J., and P. Holmes, 1983: *Nonlinear Oscillations, Dynamical Systems and Bifurcations of Vector Fields.* Springer-Verlag, 459 pp.

Hayashi, Y., 1970: A theory of large-scale equatorial waves generated by condensation heat and accelerating the zonal wind. *J. Meteor. Soc. Japan,* **48,** 140–160.

Hendon, H. H., 1988: A simple model of the 40–50 day oscillation. *J. Atmos. Sci.,* **45,** 569–584.

Hirsch, C., 1988: *Numerical Computation of Internal and External Flows.* Vol. 1, *Fundamentals of Numerical Discretization.* John Wiley and Sons, 515 pp.

Holmström, I., 1963: On a method for parametric representation of the state of the atmosphere. *Tellus,* **15,** 127–149.

Kleeman, R., 1991: A simple model of the atmospheric response to ENSO sea surface temperature anomalies. *J. Atmos. Sci.,* **48,** 3–18.

Lau, K.-M., and L. Peng, 1987: Origin of low-frequency (intraseasonal) oscillations in the tropical atmosphere. Part I: Basic theory. *J. Atmos. Sci.,* **44,** 950–972.

Lin, J. W., J. D. Neelin, and N. Zeng, 2000: Maintenance of tropical intraseasonal variability: Impact of evaporation–wind feedback and midlatitude storms. *J. Atmos. Sci.,* in press.

Lindzen, R., 1974: Wave-CISK in the tropics. *J. Atmos. Sci.,* **31,** 156–179.

——, and S. Nigam, 1987: On the role of sea surface temperature gradients in forcing low level winds and convergence in the Tropics. *J. Atmos. Sci.,* **44,** 2418–2436.

Manabe, S., and R. F. Strickler, 1964: Thermal equilibrium of the atmosphere with a convective adjustment. *J. Atmos. Sci.,* **21,** 361–385.

——, J. Smagorinsky, and R. F. Strickler, 1965: Simulated climatology of a general circulation model with a hydrological cycle. *Mon. Wea. Rev.,* **93,** 769–798.

McWilliams, J. C., 1980: An application of equivalent modons to atmospheric blocking. *Dyn. Atmos. Oceans,* **5,** 43–66.

Moorthi, S., and M. J. Suarez, 1992: Relaxed Arakawa–Schubert: A parameterization of moist convection for general circulation models. *Mon. Wea. Rev.,* **120,** 978–1002.

Neelin, J. D., 1997: Implications of convective quasi-equilibrium for the large-scale flow. *The Physics and Parameterization of Moist Atmospheric Convection,* R. K. Smith, Ed., Kluwer Academic Publishers, 413–446.

——, and I. M. Held, 1987: Modelling tropical convergence based on the moist static energy budget. *Mon. Wea. Rev.,* **115,** 3–12.

——, and J.-Y. Yu, 1994: Modes of tropical variability under convective adjustment and the Madden–Julian oscillation. Part I: Analytical results. *J. Atmos. Sci.,* **51,** 1876–1894.

Ockert-Bell, M. E., and L. Hartmann, 1992: The effect of cloud type on earth's energy balance: Results for selected regions. *J. Climate,* **5,** 1157–1171.

Randall, D. A., and D.-M. Pan, 1993: Implementation of the Arakawa–Schubert cumulus parameterization with a prognostic closure. *The Representation of Cumulus Convection in Numerical Models of the Atmosphere, Meteor. Monogr.,* No. 46, Amer. Meteor. Soc., 137–144.

Reynolds, R. W., 1988: A real-time global sea surface temperature analysis. *J. Climate,* **1,** 75–86.

Rodwell, M. J., and B. J. Hoskins, 1996: Monsoons and the dynamics of deserts. *Quart. J. Roy. Meteor. Soc.,* **122,** 1385–1404.

Seager, R., and S. E. Zebiak, 1994: Convective interaction with dynamics in a linear primitive equation model. *J. Atmos. Sci.,* **51,** 1307–1331.

——, and ——, 1995: Simulation of tropical climate with a linear primitive equation model. *J. Climate,* **8,** 2497–2520.

Selten, F. M., 1997: Baroclinic empirical orthogonal functions as basis functions in an atmospheric model. *J. Atmos. Sci.,* **54,** 2099–2114.

Song, Y., and D. Haidvogel, 1994: A semi-implicit ocean circulation model using a generalized topography-following coordinate system. *J. Comput. Phys.,* **115,** 228–244.

Staniforth, A. N., and R. W. Daley, 1977: A finite-element formulation for the vertical discretization of sigma-coordinate primitive equation models. *Mon. Wea. Rev.,* **105,** 1108–1118.

Stevens, B., D. A. Randall, X. Lin, and M. T. Montgomery, 1997: On large-scale circulations in convecting atmospheres—Comment. *Quart. J. Roy. Meteor. Soc.,* **123,** 1771–1778.

Stevens, D. E., and R. S. Lindzen, 1978: Tropical wave-CISK with a moisture budget and cumulus friction. *J. Atmos. Sci.,* **35,** 940–961.

Sui, C.-H., and K.-M. Lau, 1989: Origin of low-frequency (intraseasonal) oscillations in the tropical atmosphere. Part II: Structure and propagation by mobile wave-CISK modes and their modification by lower boundary forcings. *J. Atmos. Sci.,* **46,** 37–56.

Wang, B., 1988: Dynamics of tropical low-frequency waves: An analysis of the moist Kelvin wave. *J. Atmos. Sci.,* **45,** 2051–2065.

——, and T. Li, 1993: A simple tropical atmosphere model of relevance to short-term climate variations. *J. Atmos. Sci.,* **50,** 260–284.

——, and ——, 1994: Convective interaction with boundary-layer dynamics in the development of a tropical intraseasonal system. *J. Atmos. Sci.,* **51,** 1386–1400.

Webster, P. J., 1981: Mechanisms determining the atmosphere response to sea surface temperature anomalies. *J. Atmos. Sci.,* **38,** 554–571.

Xie, P., and P. A. Arkin, 1996: Analyses of global monthly precipitation using gauge observations, satellite estimates, and numerical model predictions. *J. Climate,* **9,** 840–858.

Yanai, M., and R. H. Johnson, 1993: Impacts of cumulus convection on thermodynamic fields. *The Representation of Cumulus Convection in Numerical Models of the Atmosphere, Meteor. Monogr.,* No. 46, Amer. Meteor. Soc., 39–62.

Yano, J.-I., and K. Emanuel, 1991: An improved model of the equatorial troposphere and its coupling with the stratosphere. *J. Atmos. Sci.,* **48,** 377–389.

Yu, J.-Y., and J. D. Neelin, 1994: Modes of tropical variability under convective adjustment and the Madden–Julian oscillation. Part II: Numerical results. *J. Atmos. Sci.,* **51,** 1895–1914.

——, and ——, 1997: Analytic approximations for moist convectively adjusted regions. *J. Atmos. Sci.,* **54,** 1054–1063.

——, C. Chou, and J. D. Neelin, 1998: Estimating the gross moist stability of the tropical atmosphere. *J. Atmos. Sci.,* **55,** 1354–1372.
Zebiak, S. E., 1986: Atmospheric convergence feedback in a simple model for El Niño. *Mon. Wea. Rev.,* **114,** 1263–1271.
Zeng, N., 1998: Understanding climate sensitivity to tropical deforestation in a mechanistic model. *J. Climate,* **11,** 1969–1975.
——, and J. D. Neelin, 1999: A land–atmosphere interaction theory for the tropical deforestation problem. *J. Climate,* **12,** 857–872.
——, R. E. Dickinson, and X. Zeng, 1996: Climatic impact of Amazon deforestation—A mechanistic model study. *J. Climate,* **9,** 859–883.
——, ——, C. Chou, J. W.-B. Lin, and H. Su, 1999: Climate and variability in a quasi-equilibrium tropical circulation model. *General Circulation Modeling: Past, Present, and Future,* D. A. Randall, Ed., Academic Press, in press.
——, ——, and ——, 2000: A quasi-equilibrium tropical circulation model—Implementation and simulation. *J. Atmos. Sci.,* **57,** 1767–1796.